UNIMORE
UNIVERSITÀ DEGLI STUDI DI
MODENA E REGGIO EMILIA

UNIVERSITÀ DEGLI STUDI DI MODENA E REGGIO EMILIA

Dipartimento di Ingegneria Enzo Ferrari

Corso di Laurea Magistrale in

Ingegneria del Veicolo

REVERSE ENGINEERING OF A ROLLS-ROYCE MERLIN CYLINDER HEAD

RETRO TRACK & AIR (U.K.) Ltd

Laureando:
FRANCESCO NONIS
Matricola 192651

Relatore:
Prof. STEFANO FONTANESI
Tutor:
CALUM E.DOUGLAS FRAeS

A. A. 2024 / 2025

Abstract

The main subject of this thesis is "Reverse Engineering," aiming to identify, specify, and explain all the techniques used to create 3D models faithful to original components when replacement parts are unavailable on the market.

In this specific case, the cylinder heads for the Rolls-Royce Merlin were produced—the famous engine that powered the Spitfire, Hurricane, and Lancaster between approximately 1935 and 1950. This engine is often defined as the one that "won the war" thanks to its formidable reliability. Curiously, the engine's history derives from the American "Curtiss D12," developed in the early 1930s in the United States before the British Air Ministry entrusted Rolls-Royce with the task of creating an engine with the same architecture but equipped with a supercharging system, as well as other fundamental modifications and improvements introduced later.

Moving to the explanation of the project itself: as is known, performing "Reverse Engineering" presupposes having access to original drawings, which, fortunately, were available. However, these alone are often insufficient, as certain dimensions or measurements may not be reported, are forgotten, or are even redundant. For this reason, in addition to the drawings, 3D scans, a Coordinate Measuring Machine (CMM), and manual measurements were utilized to validate the model. To define such a complex model, it was also necessary to learn how to manage the correct workflow within the CAD environment, which, in this case, is NX. Since the cylinder heads had to be manufactured anew, it was also necessary to define foundry models with machining allowances and corrections suggested by "Grainger and Worrall" before the final CAD/CAM phases and associated machine tool operations.

Once the models were completely defined, a study was conducted on the configuration of the cooling system used with this engine in its application on the BBMF Hawker Hurricane, which appears unsuitable (having been modified in the past) and inconsistent with Rolls-Royce standards. These modifications continue to cause overheating and cracks, primarily between the exhaust valves—a defect that the realization of new cylinder heads aims to eliminate. To obtain graphical results, CFD simulations were performed, primarily

intended to show the difference in flow rate between Bank A and Bank B, and secondarily to show the "viscous stresses" on the walls, highlighting areas where the velocity gradient tended toward zero (failing to guarantee convective heat transfer), alongside an analysis of the flow rate through all passages present in the model. Visual streamlines were added to visualize recirculation, vortices, and stagnation zones. Finally, some solutions were proposed, which will be analyzed in the future together with an appropriate CHT analysis of the cylinder head alone to evaluate potential mechanical failures due to the interaction of heat, the aluminum block, and the steel valve seats.

Summary

1. Rolls Royce, RAF and BBMF

Rolls-Royce is perhaps one the most prestigious manufacturer name of all. The genius of Henry Royce and the flair of Charles Rolls together with their determination to make the best car in the world resulted in the immortal 40/50 Silver Ghost, whose engine led them to the manufacture of aircraft engines.

Compared to much of the British political and administrative elite, often deprived of adequate scientific preparation due to their traditionally conservative outlook, Rolls-Royce stood out as an exceptionally scientific engineering company, especially during the Second World War.

And Rolls-Royce was the most scientific of British engineering companies.

The story of how Charles Rolls and Henry Royce met is a *locus classicus* in the history books, on hotel plaques and over 11,000 webpages: how electrical engineer Henry Edmunds accompanied Charles Rolls to Manchester on a train with a dining car on the morning of 4 May 1904. They got off the train and met Henry Roycce in the Midland Hotel. As written by Edmunds “I remember we went to the Grand Central Hotel at Manchester and lunched together. I think both men took to each other at first sight and eagerly discussed the prospects and requirements of the motor industry which was then in its earliest infancy”.

Since there was no Grand Central Hotel in Manchester the most viable assumption is that the men left the train at the central station and walked into the hotel next door, wrongly called by the same Edmunds “the Grand Central”.

However, there were no such trains with a dining car arriving in time for lunch that week that stopped at Central Station.

Despite the story behind how the men met, they were pleased to be introduced to each other, and this is beyond any doubt. As Rolls said afterwards: “I could not find any English-made car I really liked…eventually however, I was fortunate enough to meet the acquaintance of Mr. Royce and in him I found the man I had been looking for for years”.

When the two met Rolls was been looking for a British-built replacement for the French-built Panhards and Peugeots he had been selling to his

acquaintances. Although he dislikes two-cylinder engines, the smooth running of the two-cylindered Royce convinced him that here was a car he could sell under his own name. They soon expanded their catalogue to three, four and even six-cylinder engines. The last one, initially designed as “40/50”, was truly desired by the same Rolls after he saw and bought a D. Napier model for the Paris-Toulose-Paris race of 1900 where he worked as a mechanic. It was described as a “remarkably smooth and flexible” and the first commercially successful.

Rolls-Royce six-cylinder engine was made up of three separately cast two-cylinder units in a line above a crankshaft, which therefore had to be too long. One of the most common issues for six-cylinder engine manufacturers were broken crankshaft and the problem, as Royce found out, lay in treating the engine as three two-cylindered engines.

Every firing stroke imparted a slight twist to the crankshaft, acting much like the winding of a spring. Because the crankshaft possessed elasticity, it would naturally resist this torsion and respond by rapidly unwinding in the opposite direction. The real danger arose at certain rotational speeds when this winding and unwinding synchronized with the crankshaft's natural resonant frequencies, causing the vibrations to amplify dangerously. While such mechanical stress was merely a nuisance in an automobile, it proved fatal in aviation where engine failure meant a certain crash. Henry Royce eventually overcame this hurdle by rethinking the engine's geometry, essentially treating the six-cylinder unit as two three-cylinder engines joined in a mirror image. By arranging the crankshaft so that cylinder 1 mirrored 6, 2 mirrored 5, and 3 mirrored 4, he ensured that the internal forces balanced each other out perfectly. This symmetry, combined with a power stroke occurring every 120 degrees of rotation, eliminated the resonance issues and achieved the legendary smooth running that defined his engines.

Figure 1: Charles Rolls and Henry Royce

A gold medal was awarded at the Paris salon. Royce was delighted to hear that the prospective buyers were impressed by the silent running and wored even harder to deliver the best cars possible.

Once the evolution, and I would say revolution, of the cars was channelled into his evolutionary “Silver Ghost”, Charles Rolls switched his attention from cars to airplanes. He correctly predicted the world acceptance of the car and did it again with aeroplanes. His prophecies were accurate, including the techniques of aerial bombing, which was the main reason that allows the Merlin to be born.

Since the 1930s, Rolls-Royce has evolved from a luxury automaker into a global leader in aerospace and ultra-luxury engineering. A defining moment was the 1930s acquisition of Bentley and the development of the Merlin engine, which powered Allied aircraft in WWII. The company’s trajectory was further transformed by Sir Stanley Hooker, who joined in 1938. As a mathematician but truly passionate of fluid dynamics he focused and developed Roll-Royce piston engines and then pioneered the jet age. Under his guidance, Rolls-Royce introduced the Welland—the UK’s first production jet engine—and later the revolutionary Pegasus for the Harrier 'Jump Jet.' Last but not least we could not mention the “Rolls-Royce/Snecma Olympus 593”, the engine which powered the legendary Concorde until 2003.

Despite financial crises in the 1970s caused by the ambitious RB211 engine project, which led to the split between the aerospace and automotive divisions, the brand’s prestige remained intact. Since BMW’s acquisition in 1998, the motor car division has seen a renaissance at Goodwood, launching icons like the Phantom. Today, Rolls-Royce continues to innovate across both sectors, from the high-performance Trent engine family in aviation to its first fully electric car, the Spectre, blending its historic mechanical legacy with a sustainable future.

2. RAF – Royal Air Force

Rolls-Royce introduction gave us the perfect opportunity to talk about one of the most important military organisations in the entire world: the Royal Air Force, usually known as RAF.

The Royal Air Force is the air and space force of the United Kingdom, British Overseas Territories and Crown Dependencies. It was established at the end of the First World War precisely on 1 April 1918 merging the Royal Flying Corps (RFC) and the Royal Naval Air Service (RNAS).

Figure 2: Logo and Badge of the RAF

After the end of the War and the consequent Allied victory, the RAF emerged as the largest air force in the world. It has always played a central role in military history, let us think about the marvellous victory in the Battle of Britain which was probably the most defining moment of all. Flying legendary fighters like the Spitfire and the Hurricane, and guided by early radar technology, they handed Hitler his first major defeat. This victory was crucial because it prevented a ground invasion of Britain and changed the course of Second World War.

During the Cold War, the RAF evolved into the Jet Age. It developed the "V-Force" (including the iconic Vulcan bomber), which served as a high-altitude nuclear deterrent. This era transformed the RAF into a high-speed, global force capable of reaching anywhere on the planet in hours.

Today, the RAF is a blend of extreme technology and global aid. While it operates cutting-edge aircraft like the Typhoon and the stealthy F-35, it also focuses heavily on humanitarian missions. Whether dropping food supplies in disaster zones or conducting search-and-rescue operations, the modern RAF remains true to its motto: *Per Ardua ad Astra*—"Through adversity to the stars."

The RAF’s main aim has always been to support the British Ministry of Defence (MOD) which are to “provide the capabilities needed to ensure the security and defence of the United Kingdom and overseas territories, including against terrorism; to support the Government's foreign policy objectives particularly in promoting international peace and security”. The RAF defines its mission as providing an agile, adaptable and highly capable air force, unmatched in professionalism and able to deliver decisive air power in support of the UK Defence Mission. This mission is guided by the RAF’s own definition of air power, understood as the ability to project force from the air and space in order to influence the behaviour of people or the course of events.

3. BBMF

The acronym “BBMF” stands for Battle of Britain Memorial Flight and, as the same name suggests, it is a unit of the RAF which has the huge task of keeping old warbirds alive.

The mission of the RAF BBMF is to maintain the priceless artefacts of Britain’s national heritage in airworthy condition in order to commemorate those who have fallen in the service of the same United Kingdom.

Figure 3: Supermarine Spitfire

The Battle of Britain Memorial Flight (BBMF) was established on 11 July 1957 at RAF Biggin Hill. Originally known as the RAF Historic Aircraft Flight, it initially comprised three PR Mk XIX Spitfires and the RAF’s last airworthy Hurricane, LF363. It was subsequently renamed the Battle of Britain Flight before receiving its current title in 1969.

Between 1959 and 1965, the Flight operated a reduced fleet consisting of one Spitfire (PM631) and one Hurricane (LF363). Today, functioning as a “museum without walls”, the BBMF preserves and flies eleven historic and irreplaceable aircraft: an Avro Lancaster, a C-47 Dakota, five Spitfires, two Hurricanes, and two de Havilland Chipmunk training aircraft.

The BBMF, as anticipated, is an operational RAF unit, fully funded by the Ministry of Defence, and its purpose is to maintain these aircraft in airworthy condition as a living tribute to those who served and sacrificed during wartime.

Figure 4: Avro Lancaster

Within the fleet we need to mention three legendary planes of the ones above which played a crucial role in the Second World War. The ones we would like to mention are the Supermarine Spitfire, the Hawker Hurricane and the Avro Lancaster since they were all powered by Rolls-Royce Merlin engines.

The first was ionic with its elliptical wings, the second was the perfect interceptor while the last, but not least, was a heavy bomber (and funny to say the only bomber operated by the RAF nowadays).

Figure 5: Hawker Hurricane

4. Rolls-Royce Merlin

We would now like to focus on which has been known as “the engine which won the war”: the legendary Rolls-Royce Merlin. In doing so we will underline his development process along the years from the early beginnings to the last and most powerful: the 100 series.

4.1 A little bit of history

To properly understand why the Rolls-Royce Merlin is such an important part of the British aviation history we have to introduce the “Schneider trophy”.

The Schneider trophy was the world most famous air races which took place in the years leading up the Second World War. It was introduced thanks to the French engineer Jacques Schneider, son of a wealthy industrial, who had developed an obsession with pushing the limit of transport technology, aircraft in particular.

Figure 6: Early Schneider trophy ‘s manifest

The rules of the race were fairly simple. A triangular course was marked out with a 50km total perimeter distance then each plane departed after an interval of roughly 15 minutes to cover seven laps, making a total race distance of 350km. The aircraft attaining the fastest average speed over the course would be the winner.

The first Schneider trophy was held in 1913, at Monaco, and it was won by a French Gnome-engined Deperdussin monoplane at an average speed of only

46 mph (74 km/h). In 1920 the average speed of the winners was already 107 mph and 340 mph in 1931.

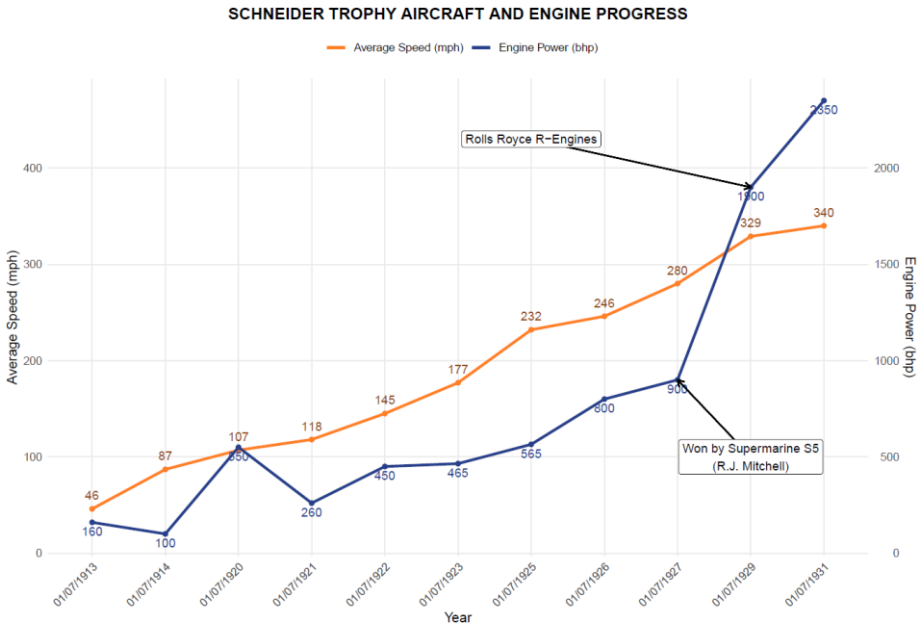

Figure 7: Schneider trophy aircraft and engine progress

By this early stage the British Government saw how important it was to the country because of the major advances introduced in mechanical construction, supercharging and fuels for example. The same Government did not lose time and set up the Royal Air Force Speed flight, tasked with providing the best military pilots to fly Britain's Schneider Trophy racers.

The first bits of Merlin were seen in the 1923 Curtiss D-12 engine, introduced by U.S. contenders which design was going to prove to be influential to both Allied and Axis sides of the next war. Instead of separated cylinders with leaky and expensive separate water jackets, each line of sic cylinders was cast into an aluminium block. This made the engine immensely rigid, light and leak-free. The two-cylinder blocks were set on a common crankcase in a V-shape at 60°, making in a V12 configuration.

Within the many British aero-engine builders there were one in particular who was truly impressed by the Curtiss D-12, the engine manufacturer Richard Fairey, noted for building elegant sharp-nosed aeroplanes which he had sold in hundreds.

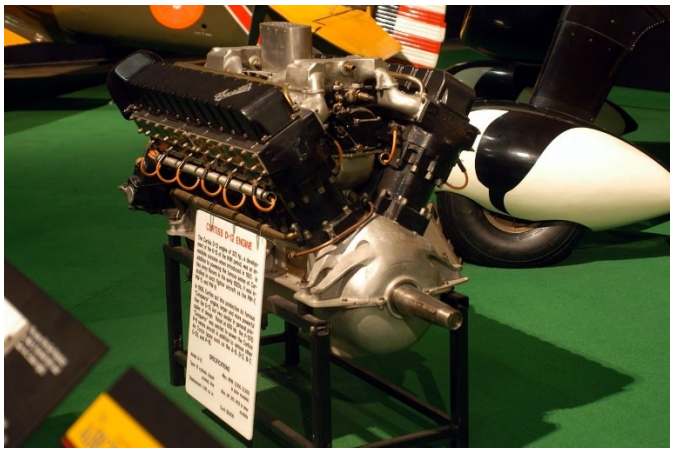

Figure 8: Curtiss D-12

He went to the U.S. to have a closer look to the same engine and what he found out was something which merged perfectly with his designs and, for that reason, he bought a licence to build it back in England.

He not just made the engine but also designed a new bomber around it: the Fairey Fox. The result was so astonishing that the same Air Ministry backed up at once since it was faster than their newest and lasted fighters. As soon as his potential was demonstrated, objecting details such as the fuel tank and the fact that it fitted an American engine, Air Chief Marshal Hugh Trenchard ordered 18 of them to equip the 12 Squadron.

Despite its success when the Air Ministry issued a new Specification for an high-performance bomber which the Fox would suit, they neglected to send a copy to Fairey, probably because the airplane was not designed to an official specification and embarrassed the same Air Ministry during annual Air Defence Exercise.

There were four major aero-engine manufacturers in England back in the days but for one reason or another the Air Ministry choose Rolls-Royce to give them something like the Curtiss D-12, but better. And so it was that Henry Royce and his team started the design of the Falcon X which became the F and then the Kestrel. And it was that engine, that enlarged by 20 per cent, that eventually became the Rolls-Royce Merlin.

Figure 9: Rolls-Royce Kestrel

4.2 Engine development

In the early 1930s, Rolls-Royce realised it needed a bigger engine than the 21-litre Kestrel, which had been performing very well in many aircraft and its only fault was to be five years old in a very fast-moving field. For this reason, the company began developing a new 1,100 hp (820 kW) engine called the PV-12. The name meant Private Venture 12-cylinder, because Rolls-Royce started the project on its own, without any government funding. The engine architecture was based on the Curtiss D-12 one: 60° V-12 27 Liters liquid-cooled engine where bore was 137.2 mm and stroke 152.4 mm. It was equipped with a single overhead camshaft (SOHC) per cylinder bank driving four valves per cylinder.

When it first runs back in 1933 the first problem were the double-helical gears reduction breaking up which were soon replaced by a stronger straight cut spur gears causing, this time, the cylinder jacket to crack. This was because Rolls Royce adopted an all-in-one aluminium cylinder blocks and the upper part of the crankcase. Rolls-Royce choose this design to allow higher crankshaft speeds and a more rigid crankcase.

In order to increase the power output, which was way lower than what was simulated, Rolls-Royce introduced the Merlin B also known as Merlin “Ramp Head”.

The transition from the experimental PV-12 to the production Merlin necessitated a fundamental departure from the original ramp head

architecture, a configuration characterized by its pent-roof combustion chamber where the inlet valves were inclined at a 45-degree angle relative to the vertical exhaust valves to induce a high-velocity "squish" effect for improved flame propagation. While theoretically efficient for combustion, this complex geometry created severe thermal gradients (often causing detonation and hot spots) and structural instabilities within the cast cylinder head, leading to chronic distortion and coolant seepage that proved catastrophic when combined with the simultaneous introduction of ethylene Glycol.

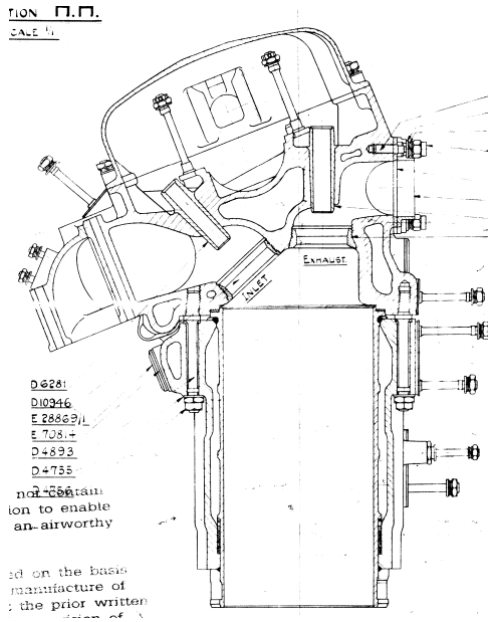

Figure 10: Merlin "Ramp Head"

The development of the Merlin saw as the next major update the division of the monoblock in three separate casting, with bolt-on cylinder heads, of the crankcase and cylinder blocks. This was renamed the Merlin "B", which first flew in the late 1935 and, with minor design changes, became the Merlin "C" powering the first Supermarine Spitfire prototype.

It was clear that the reliability of the engine was definitely not one of their key factors. For this reason, starting from the Merlin "G" (also known as Merlin "II"), the ramp head had been replaced by parallel pattern heads scaled up from the Kestrel engine. It delivered about 1030 hp in his early version.

The real "pivoting point" in Merlin development happened when Sir Stanley Hooker joined Rolls-Royce in 1938. He studied physics and mathematics,

gaining degrees and doctorate form Imperial College and then Oxford. He later became close to Theodore Von Karman, still regarded as one of the best theoretical aerodynamicists of the last century. Stanley Hooker was not an engineer but a very clever mathematician with a strong passion for fluid dynamics. Despite the fact he had not seen an internal combustion engine before joining Rolls-Royce, he was assigned to design the Merlin III supercharger. Within a week he corrected some calculations made by James "Jimmy" Ellor the leading supercharger expert for Rolls-Royce during World War II and for this reason he was placed in charge of supercharger design.

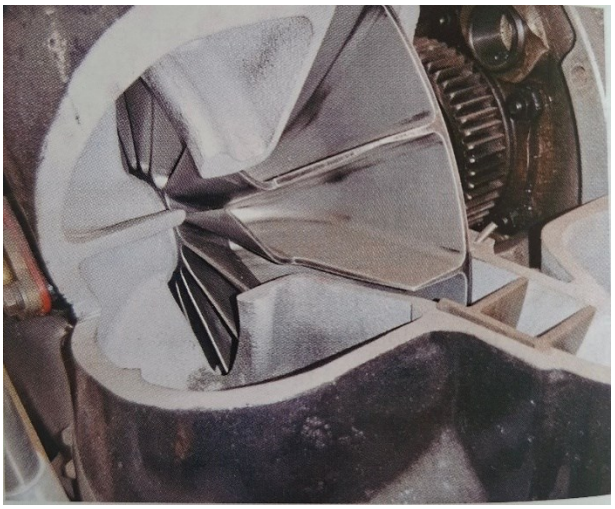

Figure 11: Rolls-Royce Merlin III supercharger – cutaway

Having studied the design of the Merin III supercharger, he had identified three main areas where he suggested that improvements could be made that would increase the efficiency of the supercharger. Increasing its efficiency reduced the temperature of the air into the engine's cylinders. This in turn increased its resistance to detonation and in theory allowed higher boost pressures to be used. The result would be higher power output and a faster fighter aircraft.

The areas Hooker outline for improvements were as follows:

- The air entering the supercharger inlet was being unduly restricted by the shape of the supercharger casing. This was a space saving solution.
- The supercharger impeller should have the tips in reduced height. This reduced the pressure re-circulation effects between each pair of blades.

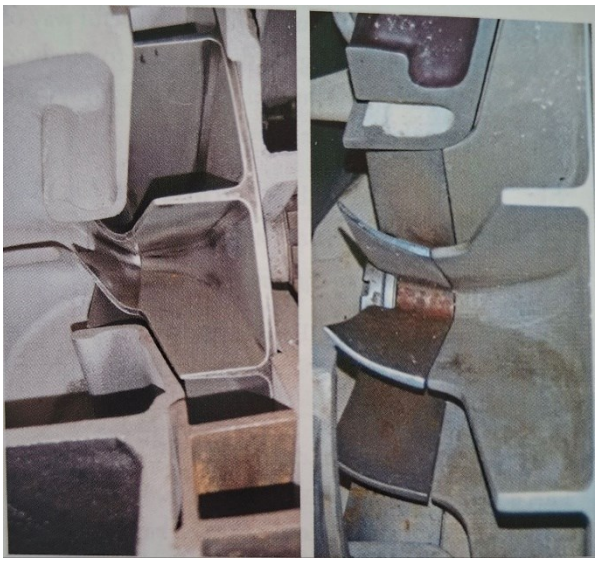

Figure 12: Hooker's reduced height impeller and Circular Arc Inducers

- The angle of the diffuser guide vanes should be altered to better match the flow direction as the flow is thrown off the tip of the spinning impeller.

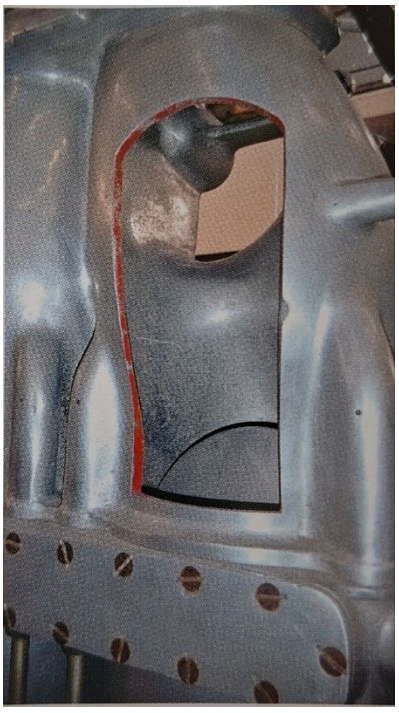

Figure 13: Hooker's "central entry" supercharger casing

Hooker’s mathematical redesign of the intake and diffuser boosted supercharger efficiency from 68% to 76%, delivering an immediate 30% power increase that saw the Merlin evolve from the 1,030 hp Merlin III (at 3000 rpm) to the 1,475 hp (at 3000 rpm) Merlin 45.

These three areas for improvements which Hooker had outlined were put into practice and resulted in the basis for the superchargers on the Merlin X, XX and 45 series engines.

In 1937–1938, Rolls-Royce saved the Merlin by "ruggedizing" it with racing technology from the R engine, turning a fragile prototype into a world-class weapon. By adopting pressurized 70/30 glycol cooling (1937), which increased the fluid boiling point to 120° allowing smaller radiators and, of course decreasing drag. Furthermore sodium-filled exhaust valves (1938) were introduced, they solved the engine's tendency to melt under massive pressure and temperature gradients, since sodium allows heat to be dissipated three times faster than solid steel.

Figure 14: Merlin's sodium filled exhaust valves

These upgrades, combined with a universal propeller shaft and successful 100-octane fuel tests, provided the thermal and mechanical "headroom" that allowed Stanley Hooker to later double the engine's power without it exploding.

The next stage development were the XX series, the first Merlin implemented with a two-speed supercharger. The extra gear increased the altitude performance of the engine significantly, as after climbing up to the height where the supercharger became ineffective (until 10000 ft) the second gear could be engaged increasing the speed of the supercharger, its pressure-ratio and allow to better maintaining maximum power at higher altitude (1240 hp at 2850 rpm at 10000 ft, 1175 hp at 2.850 rpm at 17500 ft). Merlin XX was also the first Merlin engine produced by Packard Motor Car Company as V-1650-1.

We last mention what was Rolls-Royce's most crucial project of the Second World War: the development of a two-stage centrifugal supercharger with water-intercooling introduced in the Merlin 61 engine, the successor of the Merlin XX.

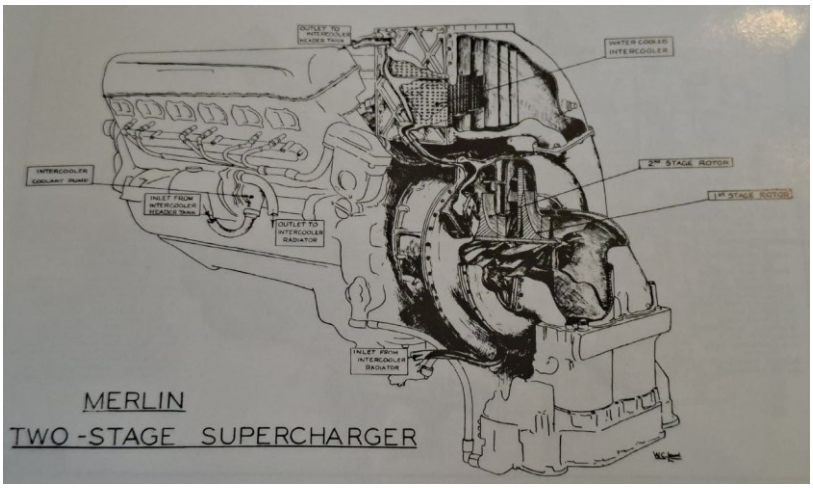

Figure 15: Merlin 61 two-stage supercharger system

Further improvements during the War were introduced with the 100 series (designation numbers swapped from Roman numbers to Arabic ones to identify war production engines) where "cross-bolted" main bearings were fundamental to prevent the crankshaft from being literally pushed out of the bottom of the engine because of the massive boost pressures. The 130 series cancelled out torque introducing counter-rotating crankshaft.

We now compare the first prototype "PV-12" with the latest "130/131" series.

Engine	PV-12 (1933)	Merlin 130/131 (1945)
Max Power	740 hp	2070 hp (over 2300 hp in tests)
BMEP	150 psi (10,3 bar)	400 psi (27,6 bar)
Supercharger	Single-stage single-speed	Two-stages, two-speeds
Boost Pressure	+2.5 PSI in (0,17 bar)	+25 PSI in (2 bar)

Cooling	Evaporative	High pressure 70/30 water-glycole
Dry Weight	1280 lbs (580 kg)	1666 lbs (753 kg)

Post-1945, Rolls-Royce repurposed the Merlin 102 into the 500 series, shifting focus from combat performance to long-term reliability and easy maintenance. These "civilianized" engines were optimized for the rigorous schedules of commercial transport rather than the intensity of aerial warfare.

5. Why these engines are still studied nowadays

Many readers are probably wondering which is the sense of study, at the time I am writing (2026), these eighty-years old engines. That is a legitimate question. But let us focus on what engineers, back in 1945, achieved with their high level of education and mathematics knowledge, hand drawings and, of course, many “mistakes”.

In just ten years piston engines developed too fast even for nowadays standard when, to achieve the same level of technology, we would probably need fifty years or more. Not because we cannot but, probably, because we do not need to.

Topics such as Fluid-Dynamics, Metallurgy and heat transfer and Mass production engineering would probably not exist as we all know.

For these reasons we would like to bring some examples widely used in nowadays racing engines which have been forgotten until the research of perfection and performance made the engineers to find out something “different”.

5.1 DB-601 A lightweight crankshaft

In May 1941, engineers at RAE (Royal Aeronautical Establishment) were studying a drowned Bf109s engines, the DB-601 A.

There was one component they carefully analysed: the crankshaft. This had some kind of lightweight features as the cranks of many aero-engines from the same period but was definitely more refined.

The DB-601 A developed a very clever method to save even more weight from the engine using barrel-shaped pockets inside the same big ends pin. The hole was then closed plugging in steel tubes which were then swagged into place at their ends. The oil flowed to the conrod bearings by passing around the periphery of the steel tubes.

This method of saving weight is still very impressive even today and it is similar to what can be found in a 2008 Formula One V8 powered Toyota RVX-08.

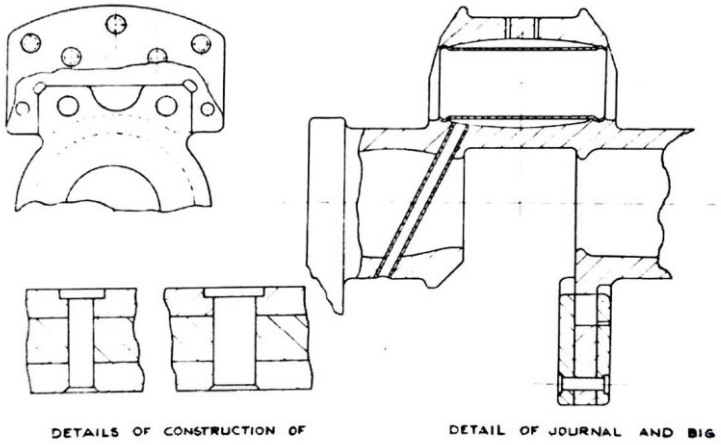

Figure 16: Detail of the DB 605 crankshaft

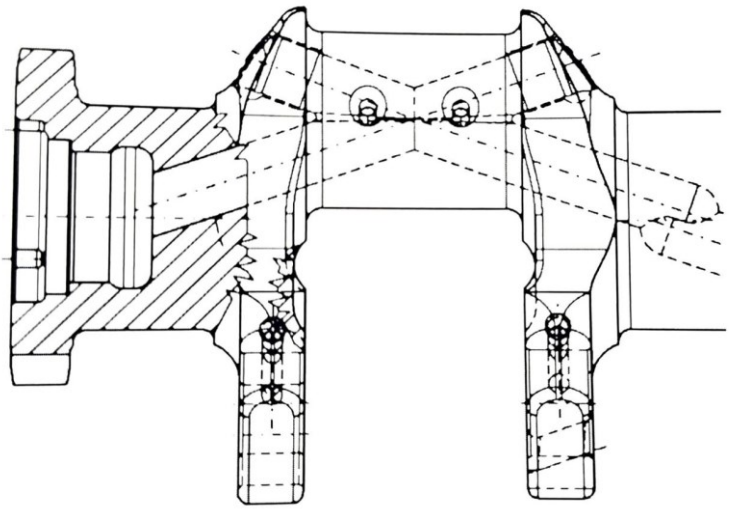

Figure 17: Toyota RVX-08 crankshaft

5.2 Jumo 213 J connecting rod

One of the latest efforts done by Jumo in the late 1945 when they developed an engine with truly racing spirit and proved to be of exceptional ambition.

Ignoring its 35 litres capacity, they decided to increase the speed not to 3000 rpm but to 4000 rpm-when usually most engines revved at about 2500-2750 rpm-giving its piston an incredible 20 m/s speed.

Jumo achieved that in the same manner a modern racing engine firm would set about it: pure science, stress and strain.

If the forces needed to be minimized but the speed had to increase, they had to decrease the mass. Unable to simply fatten up the connecting rod that

wrapped around the crankshaft pin, they decided to let the connecting rod wrap itself around the crankshaft pin. Although the thin slot with the two pins at either end simply cracked, making the lower cap into a “tension member” rather than a traditional beam to resist the bending (which needs to be more massive to do so) did work.

Its design is very similar in principle to that used in some of today’s racing engines, like the following IndyCar V8 racing engine connecting rod manufactured by the famous Cosworth in England.

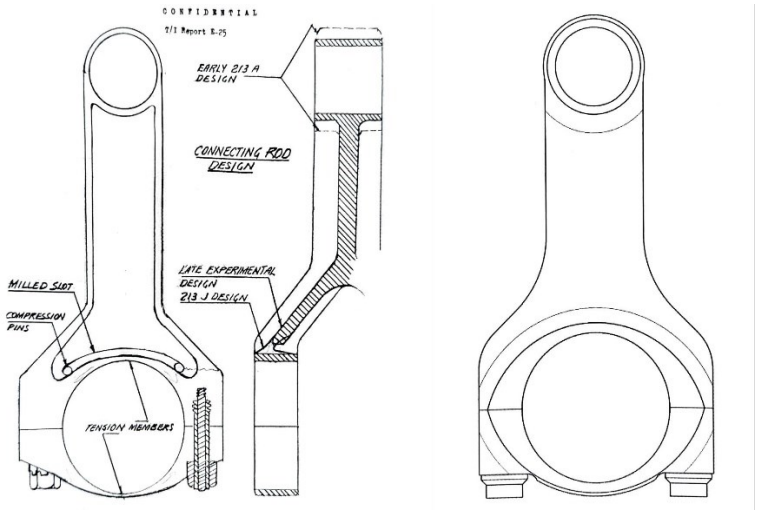

Figure 18: Jumo-213 (left) and Cosworth (right) connecting rods

The Jumo-213 was also famous because was the first water-cooled engine where oil was feeded into the end of the crankshaft. For this reason a little centrifugal air/oil separator in the crankshaft nose was implemented, still used nowadays in many high-performance racing engines.

5.3 RR 50 Hiduminium and descendents

“Hiduminium” R.R.50 is a general-purpose casting alloy developed by Rolls-Royce in the 1930s which combines excellent foundry properties with good ductility and mechanical strength.

Unlike most high strength light alloys, R.R. 50 requires only a low temperature precipitation treatment to develop the optimum properties.

This quality is particularly valuable in large castings of varying sections as internal strains, which frequently follow severe quenching, are avoided.

Casting in this alloy are not subject to age-hardening in service and the properties are well maintained at normal internal combustion engine working temperatures.

R.R. 50 was regularly employed for cylinder blocks, cylinder heads, crankcases and all parts in automobile and aircraft manufacture which demand a high standard of performance.

Here is the chemical composition:

COPPER	0.8 – 2.0 %
NICKEL	0.8 – 1.75 %
MAGNESIUM	0.05 – 0.3 %
IRON	0.8 – 1.40 %
TITANIUM	0.05 – 0.25 %
SILICON	1.50 – 2.80 %
ALUMINIUM	Remainder

While RR50 has transitioned from mainstream manufacturing to the niche world of vintage restoration, it remains a cornerstone of high-performance metallurgy. Its modern application is now centred in specialist foundries that recreate engine blocks and crankcases for historic warbirds and classic luxury motorcars. Although you won't find it in a Tesla or a Boeing 787, its legacy thrives through advanced descendants like RR58, which transitioned from the airframe of the Concorde to become the gold standard for modern Formula 1 and NASCAR pistons. Furthermore, RR350 remains a critical reference in aerospace turbine documentation for its ability to maintain dimensional stability in the extreme heat of jet engines.

6. What does “Reverse engineering” mean

Reverse engineering is the sophisticated process of deconstructing a product, device, or system to uncover its internal logic, design, and construction, particularly when original blueprints or technical specifications are unavailable. By systematically disassembling physical components or analysing digital code, engineers can extract critical knowledge about how a system functions, which serves as a foundational practice across numerous high-stakes industries.

6.1 Why Reverse Engineering Matters

This methodology is indispensable for product development and manufacturing, where it allows companies to evaluate competitor designs for improvements or recreate legacy parts that are no longer in production, as Retro does to keep warbirds flying. In the digital realm, software experts utilize reverse engineering to bridge gaps between incompatible systems, develop security patches, and identify hidden vulnerabilities within complex codebases. Furthermore, it plays a vital role in forensic investigations by allowing specialists to reconstruct mechanical failures or electronic glitches to prevent future accidents.

Figure 19: Rolls Royce Merlin cylinder skirt measurements

6.2 The Standard Workflow

The process typically begins with the acquisition of the target object and, most important if available the original drawings, followed by a meticulous disassembly phase that might involve physical teardowns of hardware. During the analysis stage, specialists employ advanced tools like 3D scanners, callipers and, as mentioned previously, the original drawings.

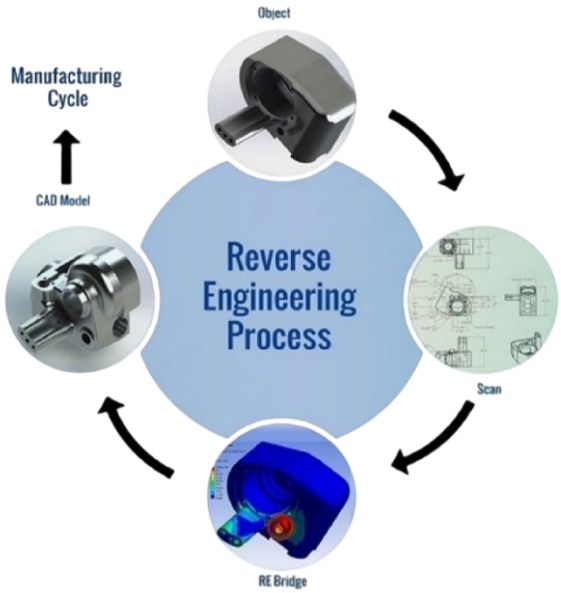

Figure 20: Reverse engineering workflow

As the design principles and engineering logic become clear, this data is often transitioned into a digital environment. Modern CAD software frequently includes dedicated tools to help transform these physical measurements into precise computer models, enabling the final phase of reconstruction where the original object can be replicated, modified, or entirely reimagined through 3D printing and modern manufacturing techniques.

Some interesting reverse engineering examples could be found in automotive industry where many companies “steal” ideas from other competitors. Could it be to copy a certain feature but, on the other hand, could be to improve something which already works well.

We now report an interesting example regarding Volkswagen and his acquisition of a Tesla model 3. It revealed that Tesla was years ahead in electronic architecture and thermal management. By tearing the car down,

competitors discovered a centralized computer system and the "Superbottle" cooling unit, which replaced dozens of redundant parts used in traditional designs. This revelation forced the entire industry to stop modifying gas-powered frames and instead develop dedicated, software-driven electric platforms to remain competitive.

Figure 21: Tesla and Volkswagen compared

7. Reverse engineering of a Rolls-Royce Merlin cylinder head

7.1 Introduction

We have now understood what “Reverse Engineering” stands for and, for this reason, we can now start to describe how Rolls-Royce Merlin cylinder head is designed again after eighty years using, in our case, Siemens NX one of the best CAD software available on the market.

The component has been chosen by the company since there are no more spare parts available on the marked and BBMF required some new ones for their engines. For these reasons will be necessary to have, at first, a casting model which will then be machined before being fitted into a proper engine.

As we already mentioned, the most important feature when we do “Reverse Engineering” is the original component. It is then usually chopped to understand how it is defined inside (think about what Volkswagen did with the Tesla Model 3) and how it is manufactured just to make a couple of suggestions.

If we now have a look at the Merlin’s cylinder head, everything seems to be quiet “easy”. But I can assure is not.

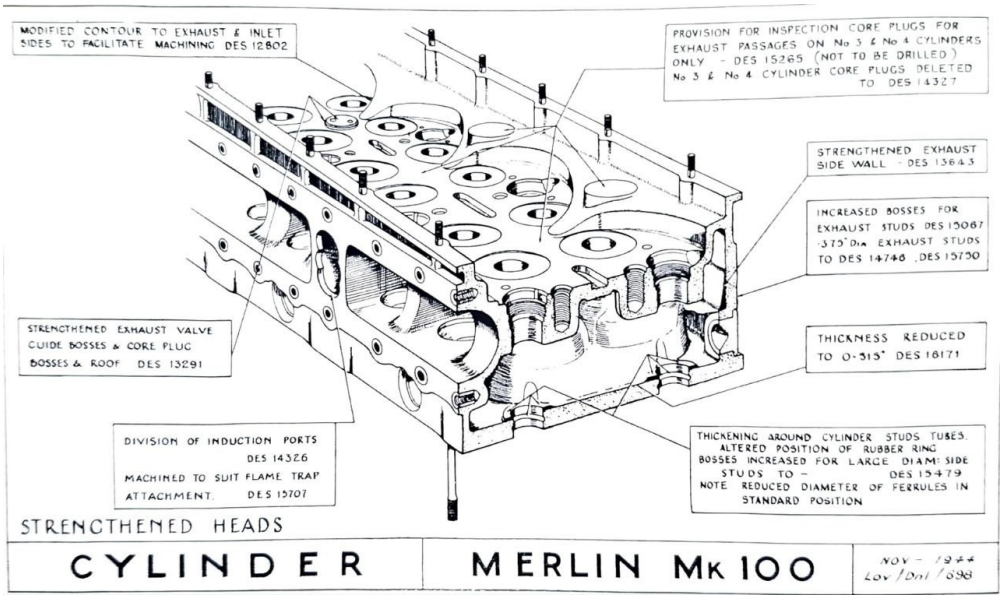

Figure 22: Rolls-Royce Merlin cylinder head detail view

We then start to analyse the component highlighting every feature just to get a general idea of what we must do. We can see from the next few photos the number of details which compose a cylinder head and why it is considered the most difficult component to be design in an engine.

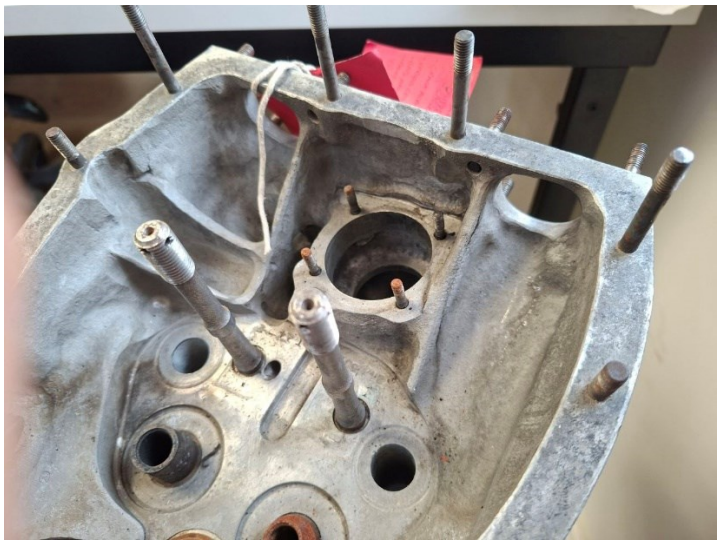

Figure 23: Cylinder head detailed view

Figure 24: Cylinder head detailed view 2

It is easy to understand how many features we need to define before having a proper manufacturing model.

Another major thing needed to complete such a huge task, if available, are the original drawings, which for components that old are usually available. Understanding them could sometimes be very challenging. Let's have a look at the following drawings from Rolls-Royce dated 1954 since has been decided to reproduce a very late cylinder head, one of the last versions ever made.

As we can see it is not easy to get all the dimensions, because of the amount of details reported and spread inside the five sheets. We then present some examples.

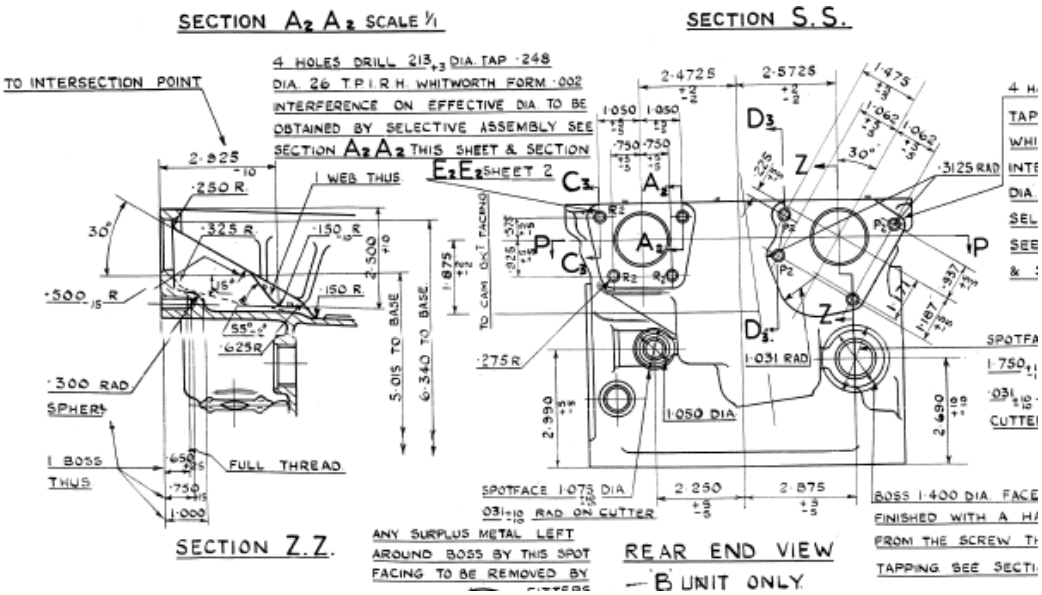

Figure 25: Drawing detail 1

It is likely that a good drawing understands take at least one entire day or even more for components as a cylinder head.

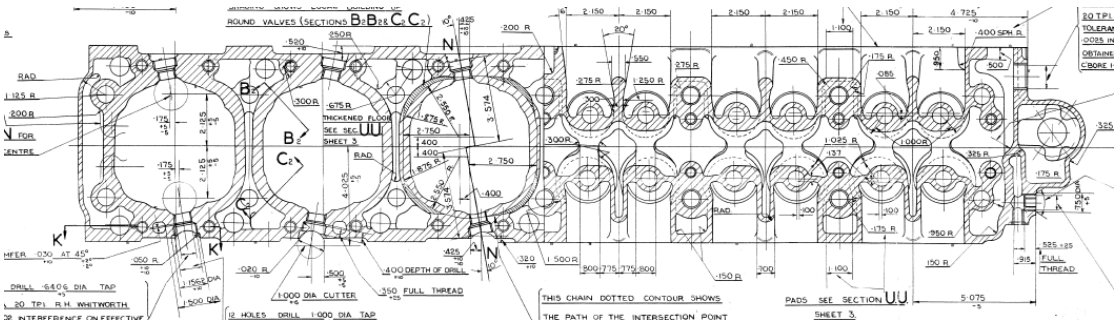

Figure 26: Drawing detail 2

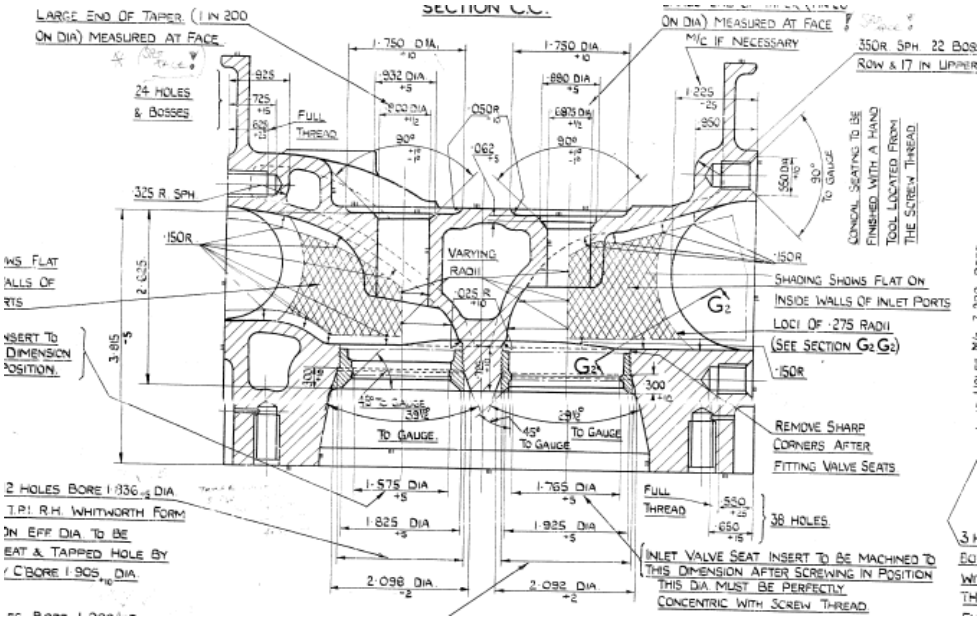

Figure 27: Drawing detail 3

7.2 Model organisation and master model

After a full understanding of the geometry and the component it is time to start modelling using every Reverse Engineering trick available because, as we will see, it is not possible to get every information from the same drawings. There will be missing features, missing dimensions and of course all the casting stocks and late machining features which are not reported.

It has been decided to split the model into four sub-models:

- A **"Master"** model: all the important construction geometries like points, axes, planes and sketches are defined. In this model we decided to include the machining bodies too which will be useful in the very late machined casting where we will be able to simply subtract them to get the final shape.
- A **"Casting master"** model: since we must reproduce both cylinder head banks, we need a proper geometry which contains all the common features between the two banks.

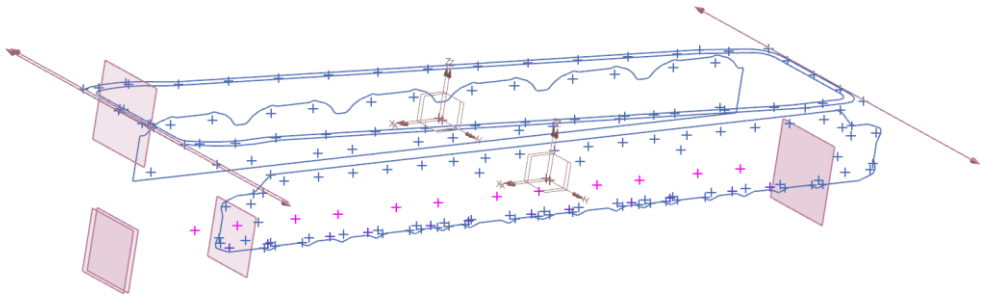

Figure 28: Envelope geometries for the model

- A **"Casting"** model: this is the geometry that will be send to the foundry and will be casted into sand. It needs to include the main geometry with all the important features that are reported into the drawings and all the casting stock material which will be then removed with machining processes.
- A **"Machined"** model: this is the last step before production. All the bodies, defined into the "Master" which replicate DFM processes are removed from the casting model obtaining the final cylinder head.

7.3 Master model

We can now describe each model in a much deeper way starting from the "Master" model.

As we anticipated the master model is also defined as "skeleton" since, in it, we define every important bit of geometry which will be later used for the part construction. This model is also needed to get a general idea of the body dimensions.

The important features inside are:

- **Locating points** such as cylinder and valve centres;
- **Planes** such as those which define the "box" inside which the model develops;
- **Axis** mostly for those features located on the cam-cover inclined profile;

- **Every “machining body” and “casting solid”** such as studs machining profiles and intake and exhaust ducts**;**
- **Bosses for the threads;**

Most features have been easily defined extracting the dimensions directly from the drawings but there are many other which are usually not clarified at all or, sometimes, even over constrained. Since we need those dimensions to recreate the geometry, we used many tools like, for example, the CMM machine also known as “Coordinate Measure Machining”.

This machine is very clever to recreate profiles using points, lines and circles. As we can see in the *Figure 29* the oil chest base geometry has not been fully constrained. We then brought the head into the machine and extrapolate the profile using two valves guides holes as a reference.

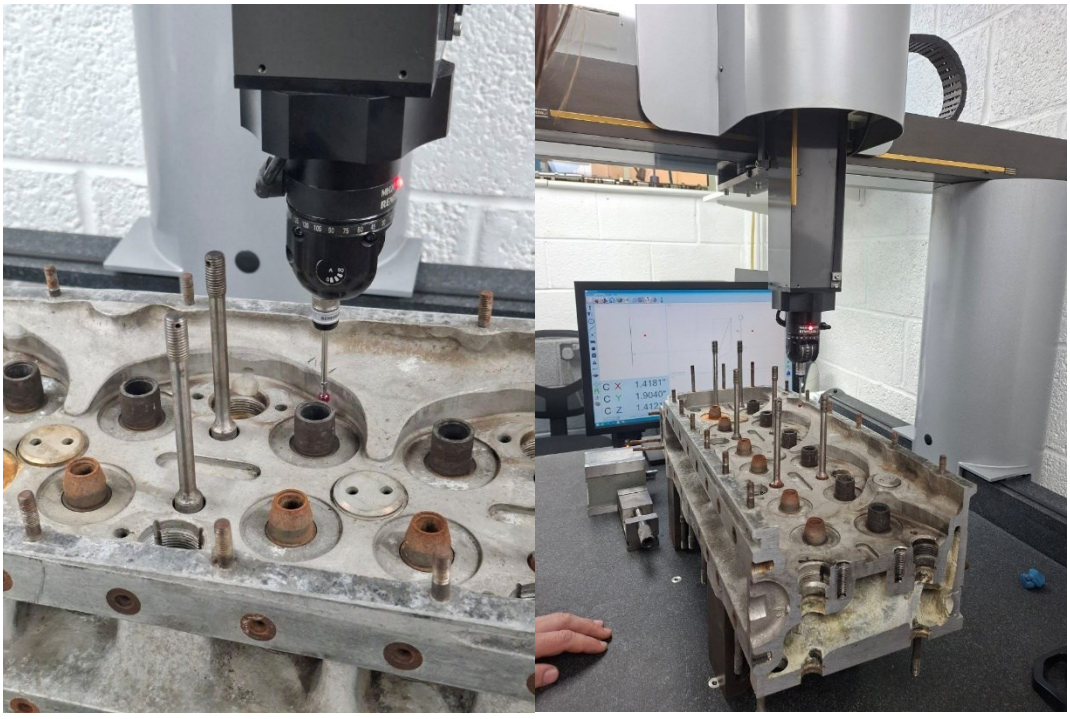

Figure 29: CMM measurments

We could extract the points and insert them inside Siemens NX to correct the actual profile.

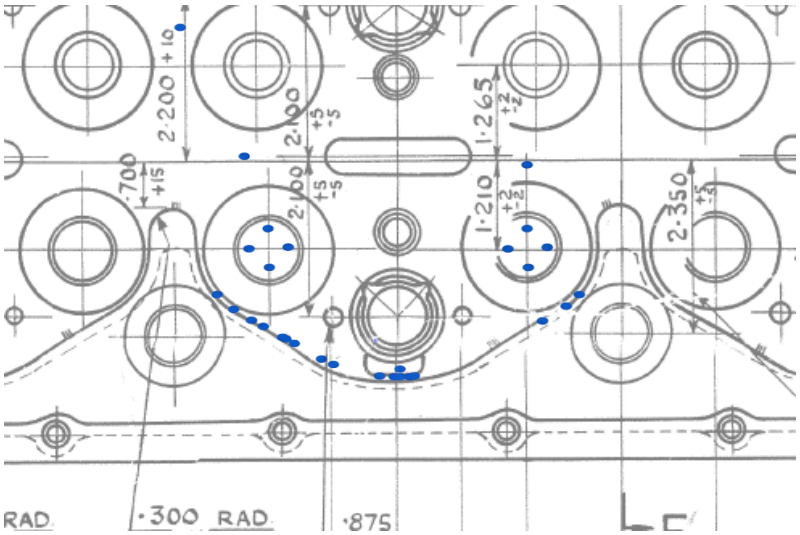

Figure 30: Coordinates overlapped to the actual drawings

Another interesting aspect, or technique, used in reverse engineering is the employ of images to recreate geometries which are not defined at all. In our project the exhaust ports dimensions have not been included into the drawing probably because, being a casting feature, designers thought that it would have been better to dimension the same ports into casting pattern drawings.

As we can see in the follow images, we recreated the same coordinate systems as in the drawing where, using a transversal view, we then add all the sections defined by Rolls-Royce.

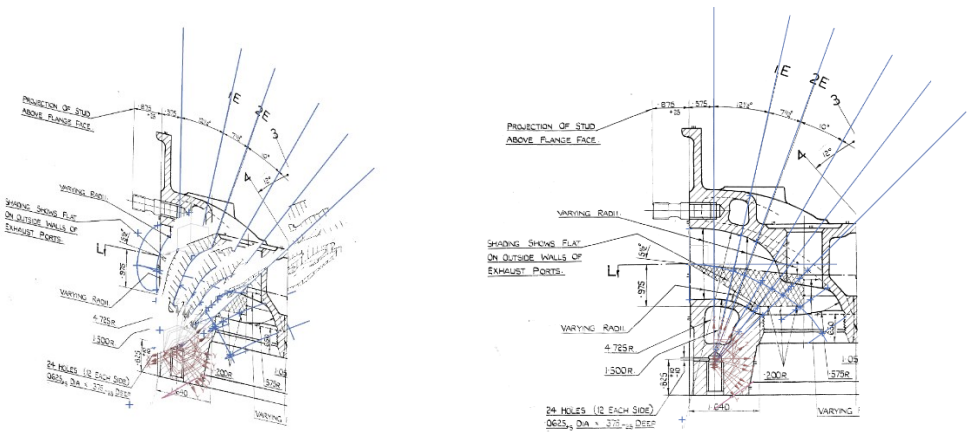

Figure 31: Exhaust ports construction

The geometry of the ports has been evaluated using an imported surface obtained from an old 3D SCAN, which will reveal very useful for many other

features in the model. Some little corrections have then been made to get a proper match between the section view and the Scan Model.

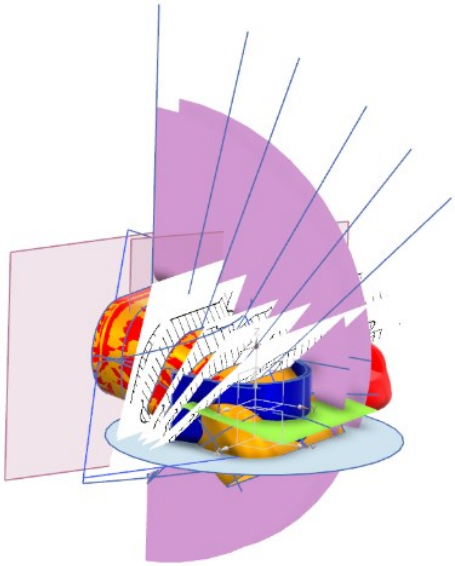

Figure 32: Exhaust ports before the final shape

One last technique we would like to mention is the comparison of different drawing because, as we said in chapter 3, the Merlin Engine has been produced under Rolls-Royce licence by Packard Motor Company in the USA and then fitted into their Mustang P51. The drawings are slightly different but, for some features, the measurements are the same. Let us think about the head total height which is not mentioned inside the Rolls-Royce but it is if we look at the Packards.

7.4 Casting Master

We can now move on to the Casting master. You are probably wondering which is the main reason of this model. Well, time saving. This is because the company has been asked to remanufacture both A and B banks which, unfortunately, are not perfectly symmetrical on the rear end. Creating a casting master allowed to have a common model, or starting point, which will then be modified to perfectly match both sides.

We started the definition of this model using all the important geometries created into the master one. This is possible thanks to a very interesting feature of Siemens NX: Product interface. With this command we are able to bring inside new models all the features previously designed into a specific position and cannot been modified or moved until the master model is updated.

The typical workflow of such a difficult model and the reason why it has been splitted into 4 different files are now easy to understand. Another important motivation is the size of the same file which has been massively reduced since we only get some feature per time.

It is now time to define both the main external and internal geometry but to be sure about these two we will use another reverse engineering technique. We now need to bring inside our model the old 3D Scan model made by Grainger&Worrall back in 2013, when the company firstly made the cylinder heads. In that occasion the heads were a perfect copy of the ones made in 1940s where all the errors inside the water jacket and outside on the external geometry are still visible. The main difference is the quality of the cast which have definitely been improved.

Although the 3D Scan have been made for the A bank we could overlapped it to our master casting anyway since the internal core is the same in both banks.

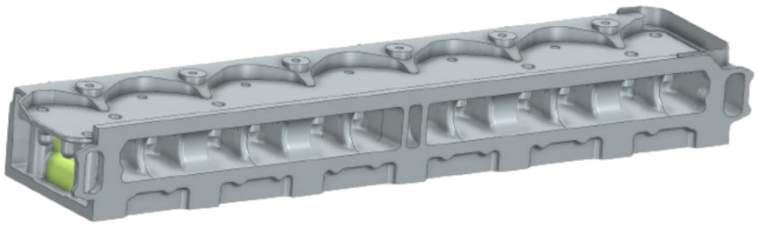

Figure 33: Casting master

This has been very helpful at first to understand the main shapes of some under constrained features and then to check that everything was in the right place with the correct dimension even though the quality is way lower as we can see from this next image.

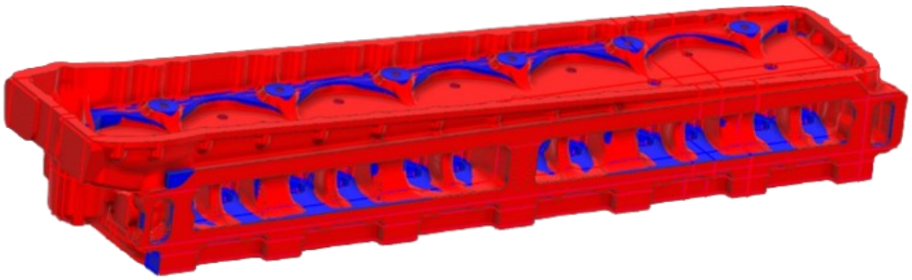

Figure 34: Model and 3D Scan comparison

Many checks have then been made bringing images in, as we already saw earlier. This was very interesting because we managed to find out many “errors” or let us call them “licensed differences” between the sections and the actual 3D model. This was probably something engineers did to reduce the number of actual views needed to represent every detail.

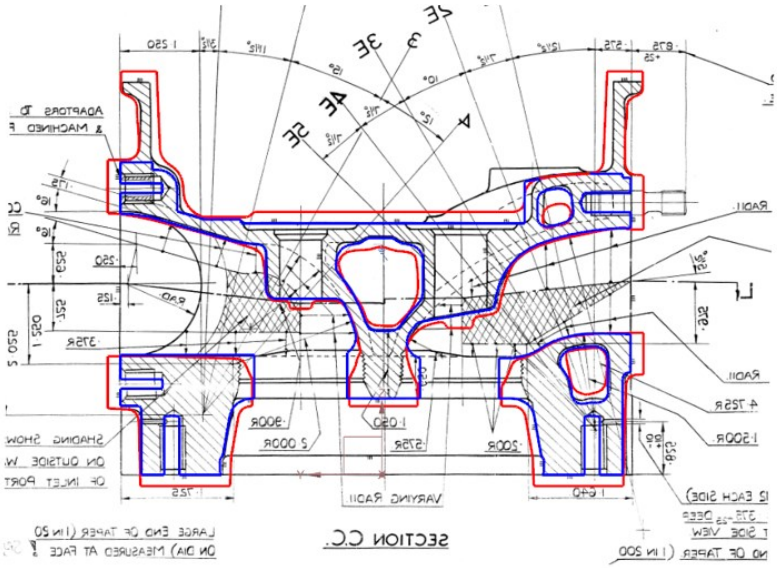

Figure 35: We can see that the hole is not in the section plane

We can see from many images how many features are similar in both the 3D Scan and our model but differ from the drawings highlighting errors made by Rolls-Royce.

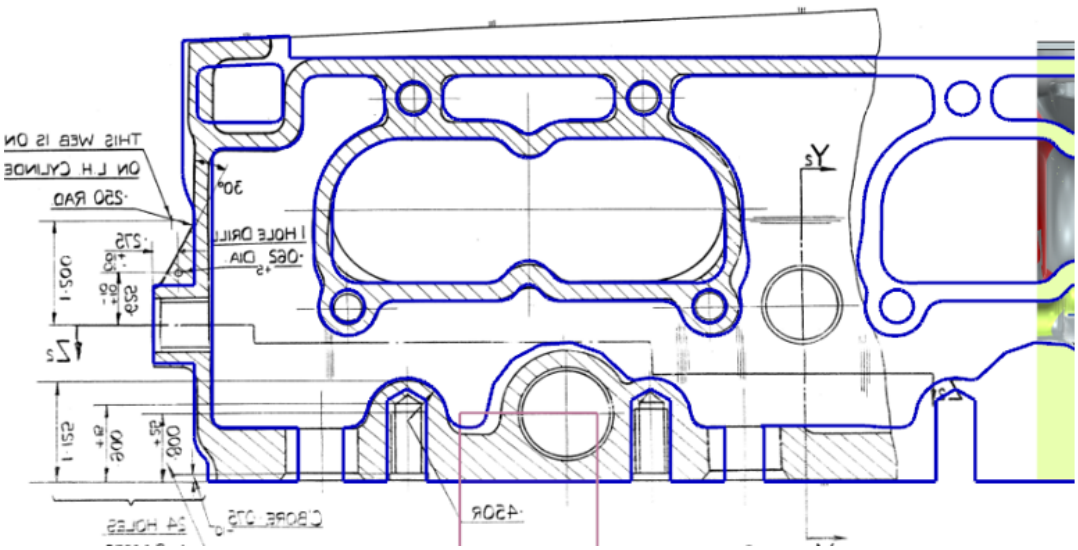

Figure 36: Differencies between the model and the Rolls-Royce drawings

Carrying on we found some different situations where our model matches the drawing but the 3D scan was different and an analysis was needed to figure out which one was the correct one. In many cases we relied on the same drawings.

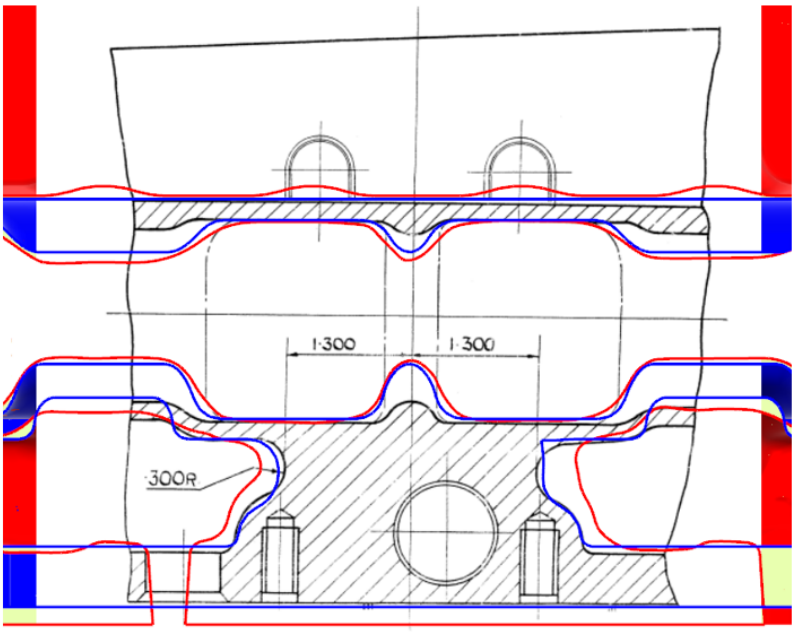

Figure 37: Wrong section in the drawings

We then need to underline an important aspect since both banks have been modelled accordingly to the original drawings. BBMF asked Retro to deliver both banks before the end of April but this, if we think about the design and manufacturing process, this was a huge problem because from our side it was

not viable to complete the models before January and, from the foundry point of view was not possible to realise all the patterns for the inlets and outlets, and the water core jacket. For this reason, a decision was made. There are some old Rolls-Royce documents which allow different component versions to be fitted into the same engine, and this rule can be extended to the same cylinder heads.

It has then been decided, with BBMF and G&W, to keep the old design of the A bank (patterns and external geometry) with a revised Water Jacket. Some corrections have been made in the zones between the combustion chambers and exhaust valves as we can see from the images below.

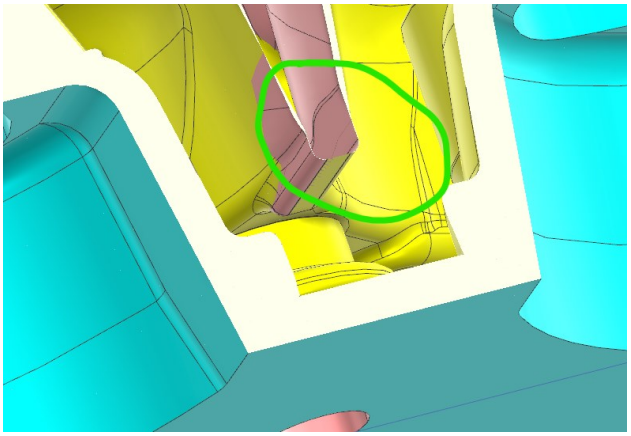

Figure 38: Important correction between the combustion chambers

The B bank will instead be made brand new from our CAD model. Both cylinder heads will be anyway useful for the further CFD simulation, which will be explained later on.

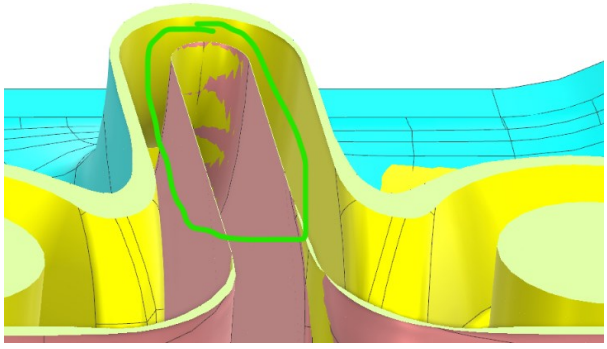

Figure 39: Important correction between the exhaust ports

7.5 Casting models

We can now move on to the casting models for both A and B bank separately. It has previously been explained why such models are so important and why we need them both even if the only B bank will be made from scratch.

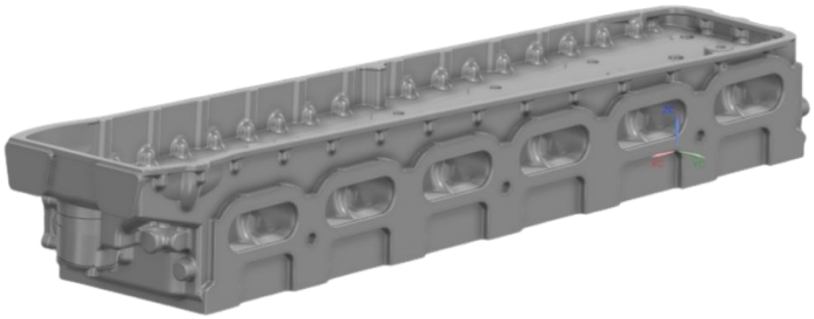

Figure 40: B bank casting model

It was than possible to complete the whole geometry adding cast material where machining processes will be applied:

- Oil chest base geometry;
- Inlet manifolds face;
- Exhaust manifolds face;
- Fireface and combustion chambers;
- Holes and oil passages in general.

This last step was crucial since, at the same time, we had to check every single detail before releasing it to the foundry.

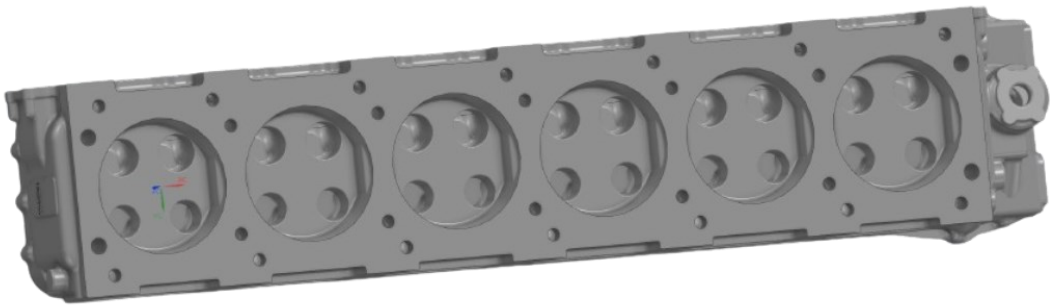

Figure 41: Detail of the fireface

After a proper geometry revision, the model was forwarded to G&W which reply suggesting some changes needed for production purposes.

As we can see from the images below, for example, the following geometries have been slightly modified.

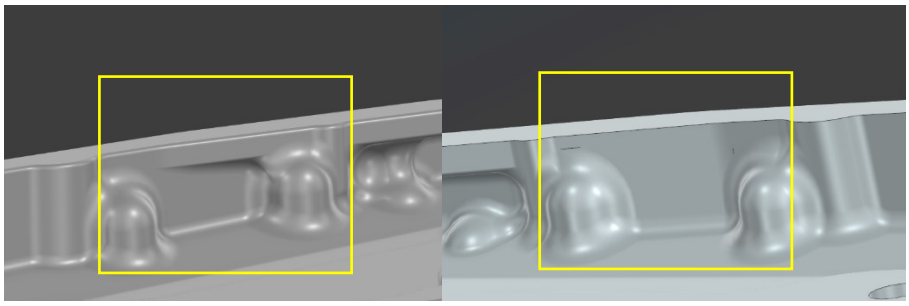

Figure 42: Examples of suggested corrections

Finally, the model was sent and the first casting came out of the factory just a couple of weeks later before being shipped on site for all the machining operations.

Figure 43: Brand new A bank out of the sand mould

7.6 Final machined model

As anticipated the model will be machined on site here at Retro and for this purpose all the solid bodies defined into the master model will finally be used since CAD/CAM technology will be applied.

This integrated workflow is essential because it eliminates the human error and slow pace of manual machining. By using CAD and CAM together, any change made to the 3D model can automatically update the manufacturing

toolpaths, ensuring extreme precision and allowing for the creation of complex, organic shapes that would be impossible to carve by hand. Furthermore, the ability to run digital simulations in CAM before cutting any material prevents expensive machine crashes and significantly reduces physical waste.

To create this last model simple Boolean operations have been made. The result is finally shown.

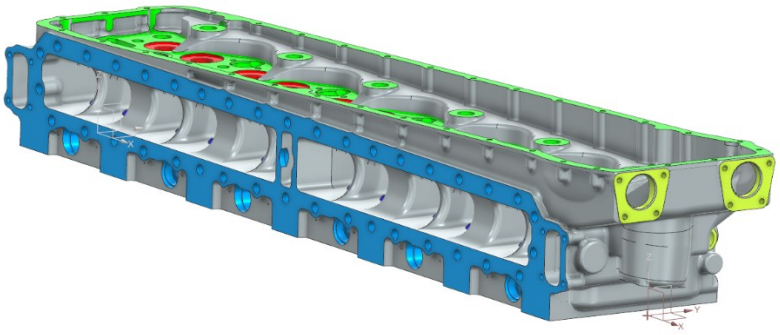

Figure 44: A Bank final model

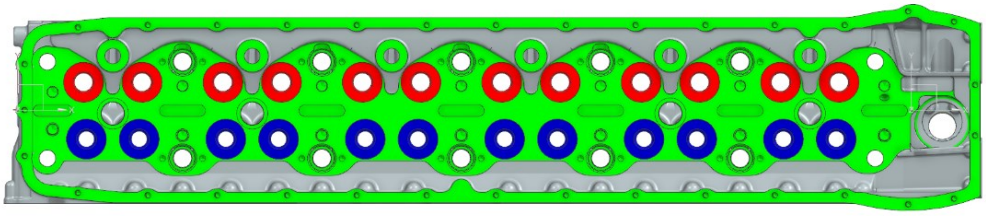

Figure 45: Oil chest base view

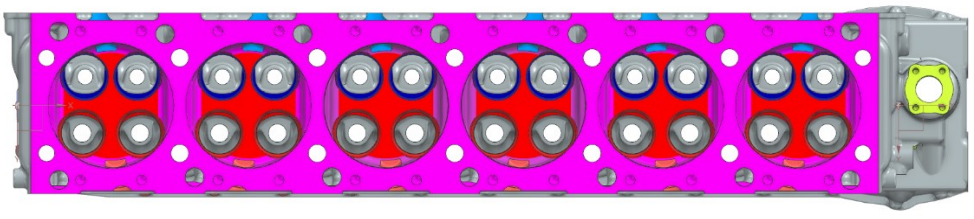

Figure 46: Fireface view

8. Water jacket flow simulation and CHT iteration with the cylinder head

8.1 System configuration

After having completed the models and sent them to the foundry it is now possible to move onto the next task. We are now going to study the flow through the cooling system. This is finalised to display and highlight problems and criticisms inside the water jacket of the engine.

This is required because after the War, due to the lack of spare parts and engines, the less complex and more reliable Merlin 500 has been installed by BBMF into their two Hawker Hurricane which were originally fitted with Merlin XX. The standard Merlin 500 features coolant outlets at the front of each cylinder head, with a rear connection for the carburettor heating jacket. However, this layout is incompatible with the Hawker Hurricane, which requires a rear-facing outlets to reach the header tank located behind the engine.

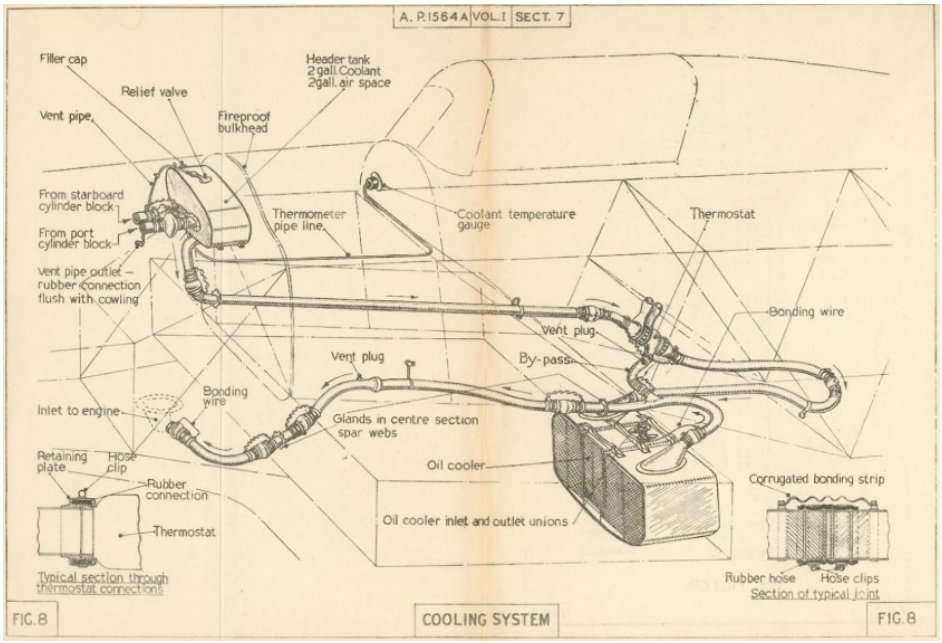

Figure 47: Detail of the Hawker Hurricane cooling system

The standard arrangement fitted to a Rolls Royce Merlin 500 is as follows. The coolant pump transfers via one external pipe on each side of the engine to the coolant rails the flow through three connections and then to the cylinder skirts. From the coolant jacket the flow enters the cylinder head via fourteen transfer

ferrules per bank. Coolant finally exits the cylinder head through the main outlets located at the front of the engine and the one at the back feeding the carburettor heating jacket.

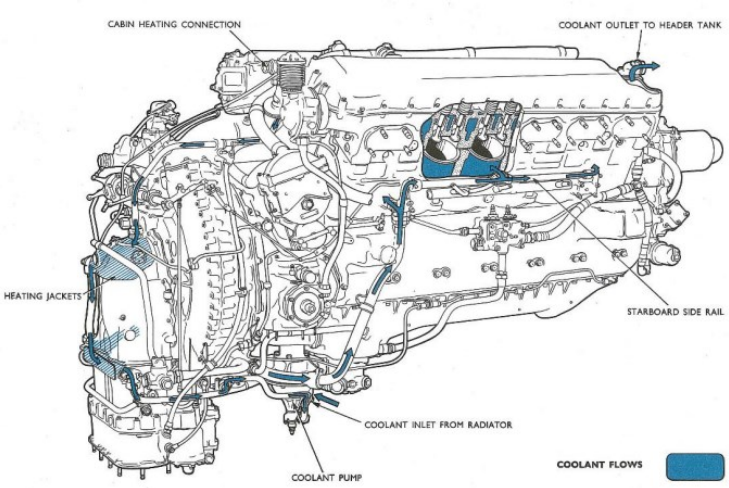

Figure 48: Merlin 500 coolant flow path

The differences between the standard Merlin 500 arrangement and that of the BBMF Hurricane impose that the front main outlets are banked off using the rear one, thanks to non-standard connections, which provides coolant flow to both the header tank (*Figure 44*) and the carburettor heating jacket. There are no further deviations of the system configuration.

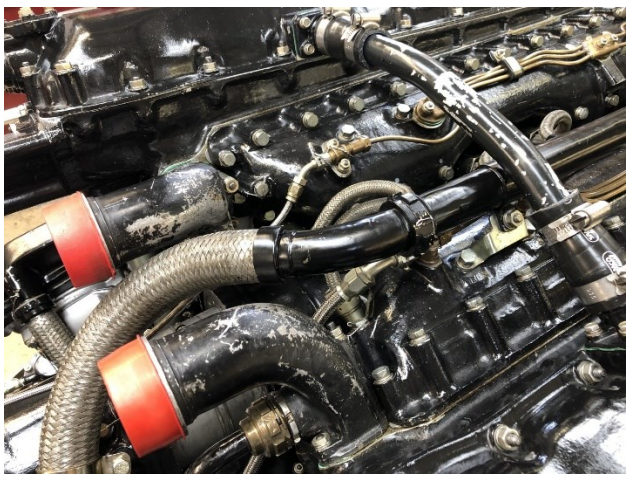

Figure 49: Hurricane's Merlin 500 with non-standard elbows (red cap)

We would like to report an interesting fact which underline how this configuration, maybe, results inappropriate and needs to be analysed properly. In the Mustang P-51H we can see front back-faced coolant elbows which

represent something between the normal 500 and the BBMF configuration and allow a proper flow through the same head where no overheat have happened.

8.2 Water jacket flow simulation

As mentioned, we are going to set a simple **flow simulation** of the whole cooling system studying the water behaviour and the Shear Stresses, which are a very useful parameter to get the velocity gradient. These highlight proper cooling regions and, on the other hand, where the fluid velocity tends to be almost zero.

The simulation will be run using FloEFD, one of the best CAD in-tool software on the market. The programme has been developed for designers which need clever results in reduced computational time to improve geometries and understand how even small changes can affect the final result. One of the best features of the software is that, being an in-tool, allows quick geometry changes with no need to export, import and redefine the geometry part as in Star-CCM+, just to make an example.

Before even thinking about setting the two simulations we had to define the complete water jacket and to do so many different mods and documents have been studied to dig out the proper geometry specifications.

One of the first thing to do was to decide the skirt configuration we want to study. As mentioned in the early beginning of the document many different versions of the Merlin have been realised through the years and many cylinder heads and skirts were made. For a better understanding of these changes, we had to dig out the Mod 700 which is a very important document where the differences between the old and the new cylinder skirts in terms of geometry and water feeding system and connection with the cylinder head are shown.

We can see the different geometries and connections made to join head and skirts together.

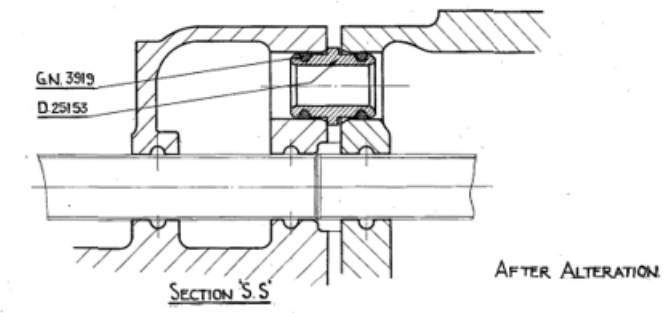

Figure 50: Post mod 700 configuration

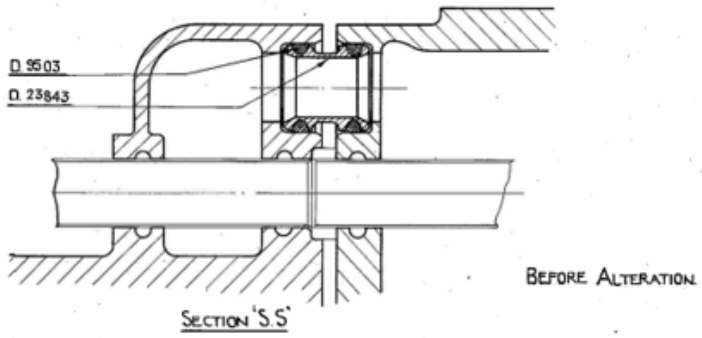

Figure 51: Pre mod 700 configuration

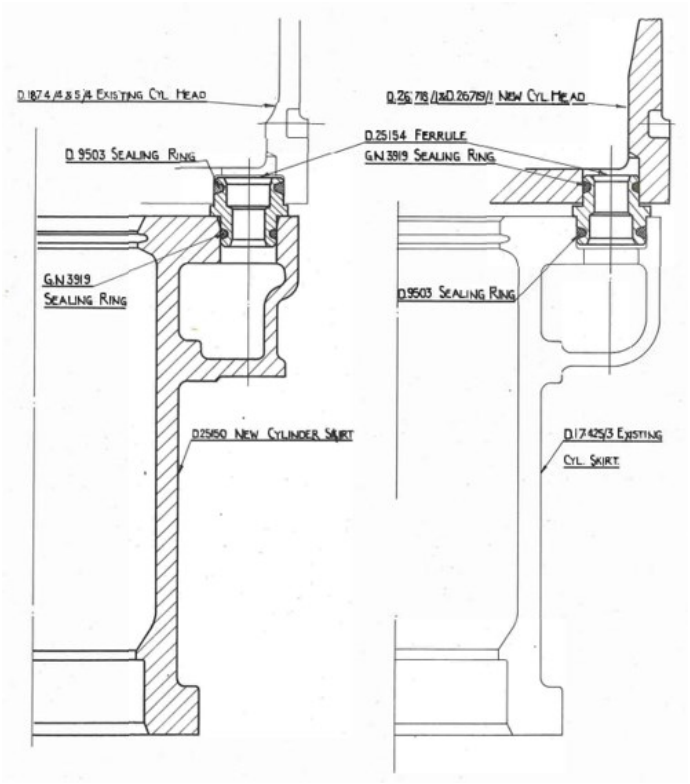

Figure 52: Hybrid configurations

The important configurations, since we designed a very late cylinder head and the Merlin 500 is the engine to simulate, are the first (*Figure 44) and the* second shown in the bottom image (*Figure 46*).

The cooling flow path and the geometry have now been understood. We can now design all the other important component in the water system which are (including the already modelled heads):

- Cylinder heads, both A and B bank;
- Cylinder skirts;
- Coolant branch inlet pipes;
- Head-Skirt connectors;
- Hurricane spec coolant outlet elbows (non standard part);
- Water pump and impeller.

It is now possible to define what we called a “space model” starting from the cylinder skirts. Unfortunately, we are not provided with the original drawings but we managed to find out the pre-mode 700 ones which have been very useful to define all the external dimensions and the relative position of the many features. Everything else was properly measured from the real post-mod skirts that we have here on site.

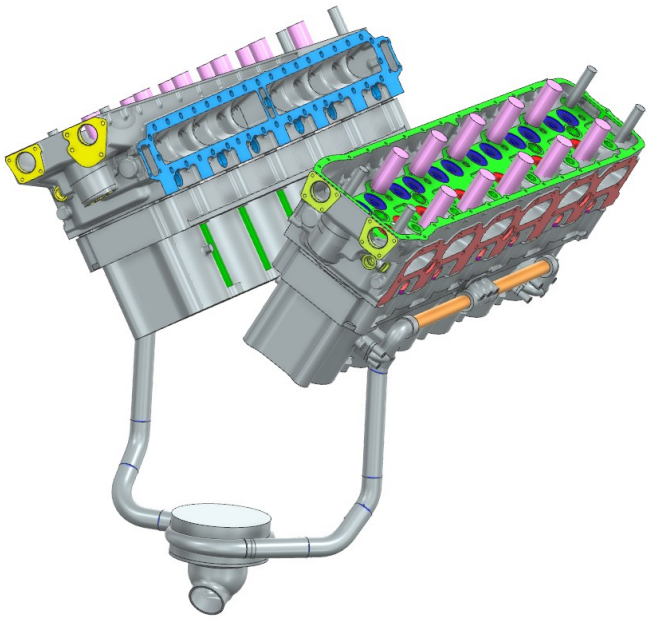

Figure 53: Complete simple assembly model

The coolant domain has then been extracted giving the following, unusual if we think about modern engines, geometry. We can see many little pockets between the cylinders with partially covered fluid passages because of the presence of the main cylinder studs.

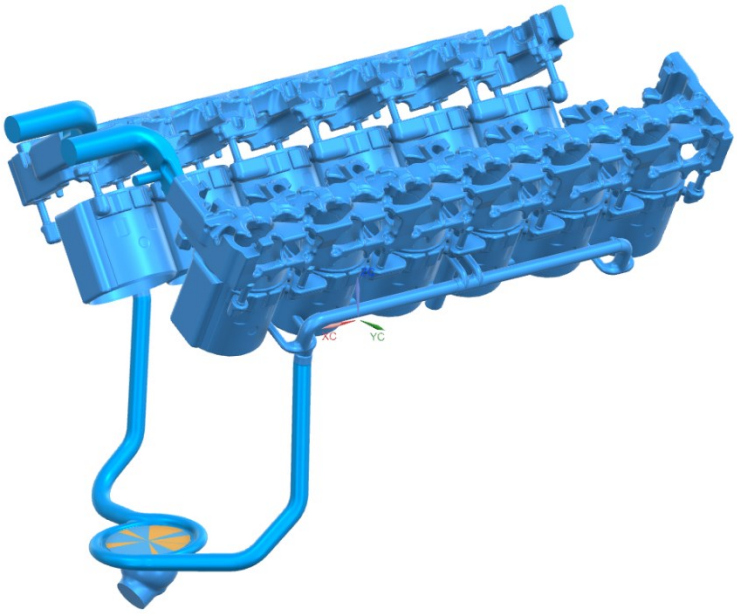

Figure 54: Hurricane's complete water jacket

Some other interesting observations are focused on the rear elbows. It is easy to visualise how this configuration could cause water stagnation on the front end of the engine due to the lack of circulation inside the head. Again, as we already mention, these are a "non-standard" component which have been fit into a Merlin 500 because the original XX series are no longer available. The manufacturing quality is also very poor as we can notice from the following images.

Figure 55: Elbows inlet section detail

It is possible to notice how badly they have been made just focusing on the inlet section, which is completely asymmetric and distorted.

8.3 Data for the simulation

The geometry is now completed and ready to be brought inside FloEFD environment but, before doing so, we need to gather all the important information to properly set the simulation such as fluid characteristic and properties, mass flow and pressure drops along the circuit. These are data available in our archive but, of course, we also had to read many historical documents. The most important of all is the TSD 83 which is an original Rolls-Royce document where *"Performance and Installation data for Merlin 24 and 500 series"* are reported.

Starting from the fluid characteristics we must underline the fact that Rolls-Royce Merlin still runs on water-glycol 70/30 mixture. Since we could not find the coolant properties for those percentages, the "Rule of Mixture" has been adopted which allows to tabulate, as the name suggests, the properties for a mixture given the volume of the components.

$$\emptyset_{mix} = \emptyset_{water} * 0.7 + \emptyset_{glycol} * 0.3$$

This simplification could be adopted since we are going to run a steady state, incompressible simulation where all the values are tabulated for a reference temperature of 100°C. This value is relatively close to the real temperature of the coolant system, little variations could then be neglected.

Water properties are easy given while the glycol's required some calculations. We then specify that BBMF nowadays uses a modern alternative to the glycol called AL39 which is, fundamentally, the antifreeze we can find in our cars.

We would like to point out that all the values have been converted to the SI unit system for a better understanding. All the conversions are as follows:

- Density (ρ) from $\frac{pound}{ft^3}$ to $\frac{kg}{m^3}$;
- Thermal conductivity (κ) from $\frac{BTU}{hr\ ft\ °F}$ to to $\frac{W}{m\ K}$;
- Specific heat coefficient (cp) from to $\frac{BTU}{lb\ °F}$ to $\frac{kJ}{kg\ K}$;

- Dynamic viscosity (μ) from cP to $\frac{kg}{m\,s}$.

The values for water and AL39 are as follow:

	Density [kg/m3]	**Thermal conductivity** [W/mK]	**Specific heat coefficient** [kJ/kgK]	**Dynamic Viscosity** [kg/ms]
Water	985.05	0.67703	4.216	0.000282
AL39 (glycol)	1042.15	0.22862	2.777	0.0004667
Mixture	983.28	0.54251	3.784	0.00033741

Carrying on we tabulated the flow circulating in the system, the pressure rise through the pump and the pressure drops in the head. These data have been extracted from many 1940s Packard's reports (see *"Bibliography"*) except for the flow moved by the pump, which is given by TSD 83.

The coolant pump is directly connected to the engine using a 3:1 ratio which, for the maximum speed considered in the analysis 3000 RPM, gives us 4500 rpm. At this velocity 122 $\frac{ImpGal}{min}$ are moved by the same. The equivalent value in the SI is 0.55462 $\frac{m^3}{min}$.

We can now extract the pressure rise using Packard's curves. Before doing so our Imperial Gallon value needs to be converted into the US equivalent which is 147 $\frac{USgal}{min}$. The charts developed by Packard are defined thanks to two non-dimensional parameters which allow to compare different pumps on the same graph. For a given temperature of 180 °F and a pump inlet pressure of 3.4 PSI we get:

$$\frac{GPM}{N\,x\,10^{-2}} = 3.2559$$

It is now possible to extract from the diagram the following:

$$\frac{\Delta P}{N^2\, x\, 10^{-6}} = 2.57$$

The pressure rise is easily given:

$$\Delta P = 52.043\ PSI$$

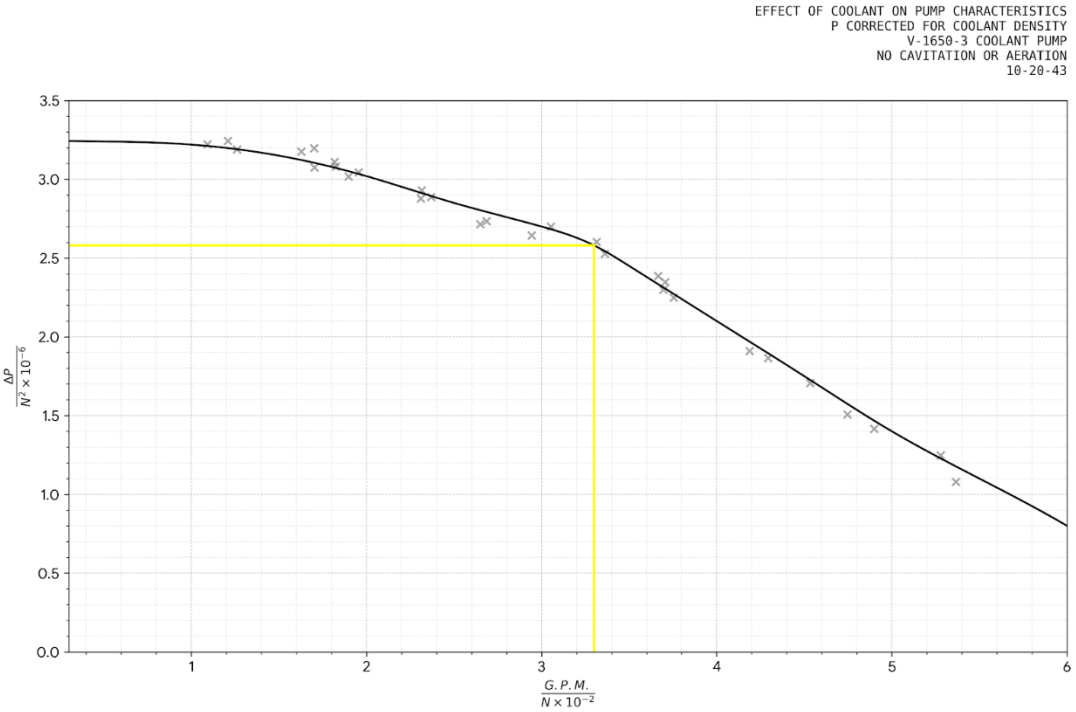

Figure 56: Pump characteristic curve

Since we know the pump inlet pressure, the outlet value is soon defined as 55.4425 PSI.

We now report all the input data in agreement to the SI:

- Inlet pressure: 23442,2 Pa;
- Outlet pressure: 382262,6 Pa;
- Fluid temperature: 355,372 K.

8.4 Pump Simulation

The simulation could now be set inside FloEFD environment. It has been decided, to reduce the computational cost, to split the domain into two different simulations. In the first one we will analyse the pump and then use the outputs to define the cylinder bank where we have the lower amount of flow. This first simulation will be used to show that the percentage of flow is not symmetric between A and B bank but, as some old Packard's report suggested, it is 47% through the B bank and 53% through the A bank.

As we mentioned above, a simple model of the pump have been developed for this purpose. The internal geometry is given thanks to some drawing from the "*Air Corps Library*" archive since the component is the same in both Packard and Rolls-Royce engines.

Figure 57: Pump Case

It is easy to understand how the right-hand side could cause restriction and reduction in the flow because of the corner which, compared to the other side, does not allow the water to exit straight but it is the reason of recirculating bubbles and flow detachment.

The impeller was also needed because even if we will run a steady-state simulation, the rotation and its dynamic effects need to be included into our

calculation. This is possible thanks to a proper boundary condition which does not need moving mesh such tools.

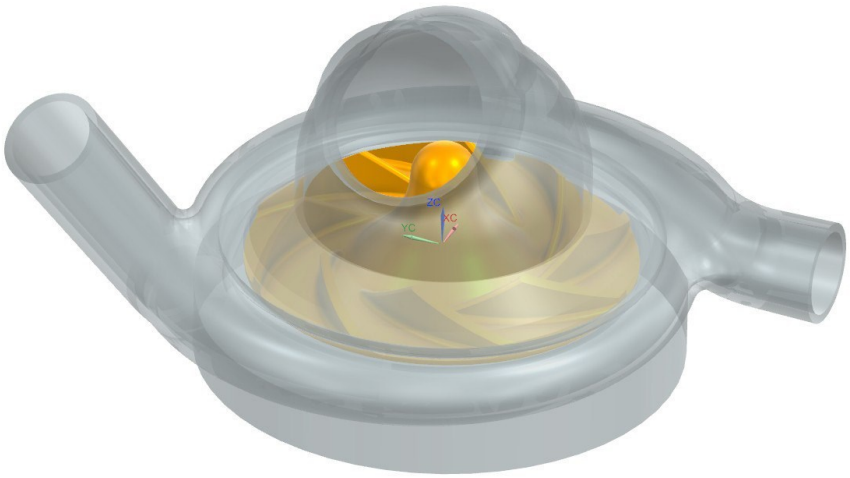

Figure 58: Model of the pump and the impeller (metti indicazioni in e out)

As mentioned, a rotating region has also been defined as follow.

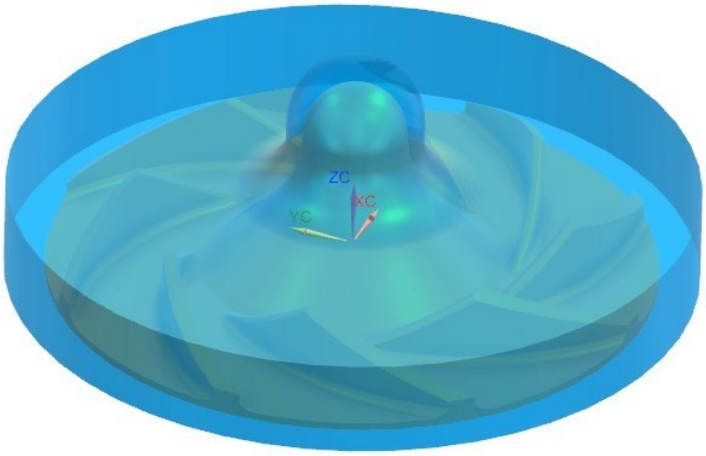

Figure 59: Rotating region

This solid will also be used to create a **finer mesh**, which will allow for more accurate calculations in that specific region.

We can now set the “**boundary conditions**” for the given simulation:

- Mass flow inlet where $\dot{m} = 9.089148\ \frac{kg}{s}$;
- Pressure outlet (both for A and B bank) where $p = 382176.4\ Pa$;
- Rotating region rotating at $w = 471.24\ \frac{rad}{s}$;

Moving to the "**initial conditions"** we identify:

- $T = 355.372\ K$;
- *Turbulent kinetic energy*

$$k = \frac{3}{2}u' = \frac{3}{2} * 0.36034 = 0.19477\ (\frac{m}{s})^2$$

Where u' is the reference velocity which definition is

$$u' = T.I. * u$$

- $T.I.$ is the "Turbolence intensity" and is assumed 0.1;
- u is the "inlet velocity" for the given mass flow.

$$u = \frac{\dot{m}}{\rho * A} = \frac{9.089148}{983.28 * \pi * \frac{0.05715^2}{4}} = 3.6034\ \frac{m}{s}$$

- *Turbulent dissipation rate*

$$\varepsilon = C_\mu^{3/4} \frac{k}{TLS}^{3/2} = 0.09^{3/4} \frac{0.19477}{0.005715}^{3/2} = 2.4714\ \frac{m}{s}$$

Where:

- TLS is the *"Turbolence length scale"* and is defined as the inlet diameter divided 10;
- C_μ is called "turbulent viscosity constant" and it is a non dimensional coefficient which relates the turbulent kinetic energy, the turbulent dissipation rate and the turbulent viscosity.

It is now possible to generate the mesh. In the first simulation has been decided to use the option "automesh" with the refinement level set to 4. Some additional improvements have been defined increasing the level of the fluid-solid boundary cells to two. This gave around 37243 cells.

The first rough mesh is then showed.

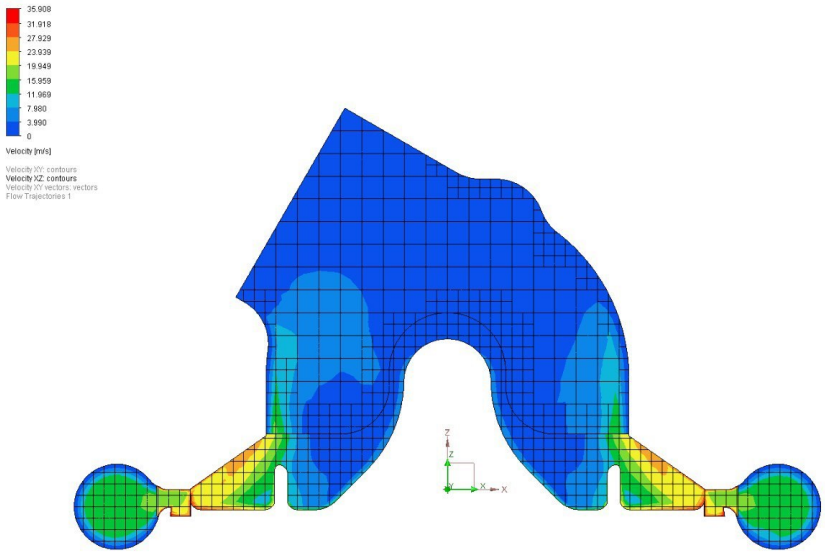

Figure 60: Mesh on plane XZ

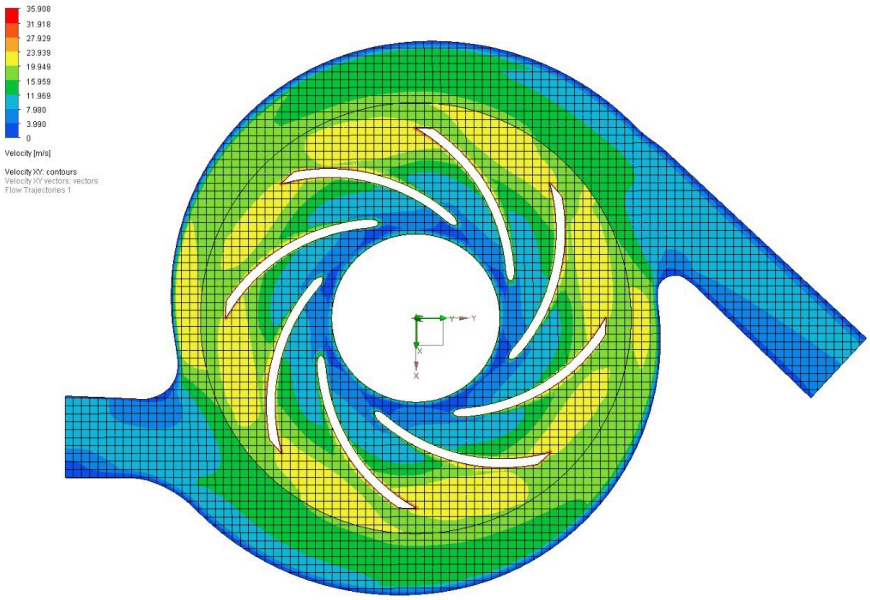

Figure 61: Mesh plane XY

As we can see this mesh was meant to obtain a first result helping the convergence of the simulation. Without any major refinement the results cannot be considered reliable. The velocity scene is also shown above and, again, the velocity gradient is not smooth at all. This forced us, as imagined, to run more simulations after this first one. All the settings are mentioned below

but we will just focus on the last and more refined one. In order we managed to run:

- **Second simulation**
  - Automesh level 4;
  - Refinement inside the rotating region with fluid cells level two and fluid-solid cells level three;
  - Stagnation points refinement with fluid cells level two and fluid-solid cells level four;
  - Total 99565 cells.
- **Third simulation**
  - Automesh level 5;
  - Refinement inside the rotating region with fluid cells level three and fluid-solid cells level three;
  - Stagnation points refinement with fluid cells level two and fluid-solid cells level four;
  - Total 306929 cells.
- **Fourth simulation**
  - Automesh level 5;
  - Refinement inside the rotating region with fluid cells level three and fluid-solid cells level three;
  - Stagnation points refinement with fluid cells level two and fluid-solid cells level four;
  - Additional refinement around the impeller blades with fluid cells level three and fluid-solid cells level four and increased number of cells in small channels (30);
  - Total 464652 cells.
- **Fifth simulation**
  - Automesh level 5;
  - Refinement inside the rotating region with fluid cells level three and fluid-solid cells level three;
  - Stagnation points refinement with fluid cells level three and fluid-solid cells level four;

- Additional refinement around the impeller blades with fluid cells level three and fluid-solid cells level four, increased number iof cells in small channels (30) and curvature set to level two;
- Total 501955 cells.

It has then decided to stop since the simulation main goal was to prove that the flow to the two banks is asymmetric as mentioned in the Packard's reports.

8.4.1 Graphic scenes

The results of this last simulation are showed below.

- **Mesh plane XY**

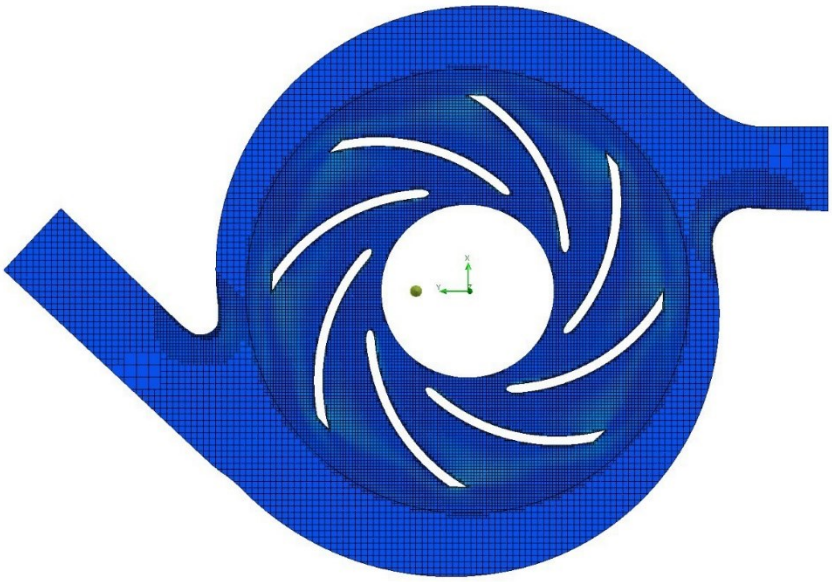

Figure 62: Mesh plane XY

In this section it is easy to notice all the refinements in the mesh, which have been defined on the two stagnation points where we have the smallest section in the channel, in the rotating region and around the blades. On the other side there are no boundary layer since Simcenter FLOEFD solves it using a 2-scale wall treatment method, which combines analytical and semi-analytical approaches within a cut-cell Cartesian mesh, allowing it to handle both thin and thick boundary layers without requiring the extremely fine mesh density typical of conventional CFD tools. This approach seamlessly bridges laminar and turbulent formulations depending on the local cell size and boundary layer

thickness. This approach is very easy but, on the other hand, does not allow to run (for example) a LowRe simulation since it is not possible to set a proper number of layers.

- **Mesh plane XZ**

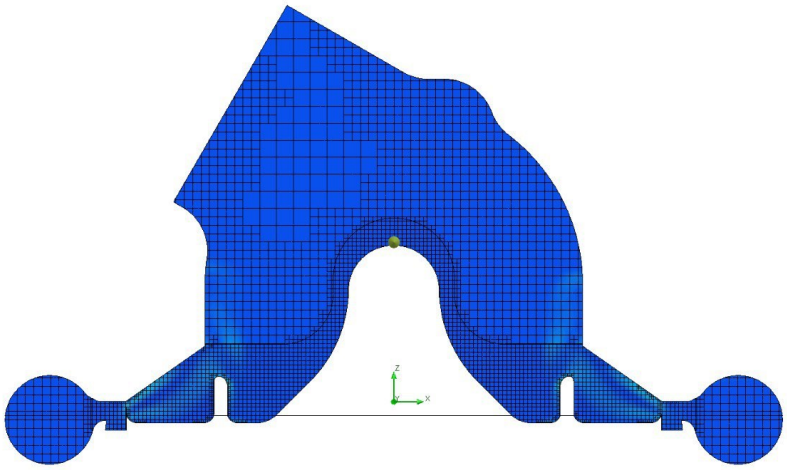

Figure 63: Mesh plane XZ

The mesh on this plane is appropriate for our simulation, on the other hand it would have been a good idea to increase the refinement level between the impeller vane and the circular passages to better analyse the velocity gradient in the rotating-static boundary. This is always very critical because it defines small errors while calculating the values in the cells. Again, since the error is lower than 1% (see below), the output values have been considered fine.

- **Velocity plane XY**

  This image is very interesting since it allows us to see the pressure rise in the vanes of the pump which is what we expected. It is then easy to notice the blades wake inside the rotating region and the related velocity gradient caused by the rotation of the same impeller.

  One last detail is the (possible) recirculating bubble on the lower (B bank) outlet identified by the large dark blue shadow.

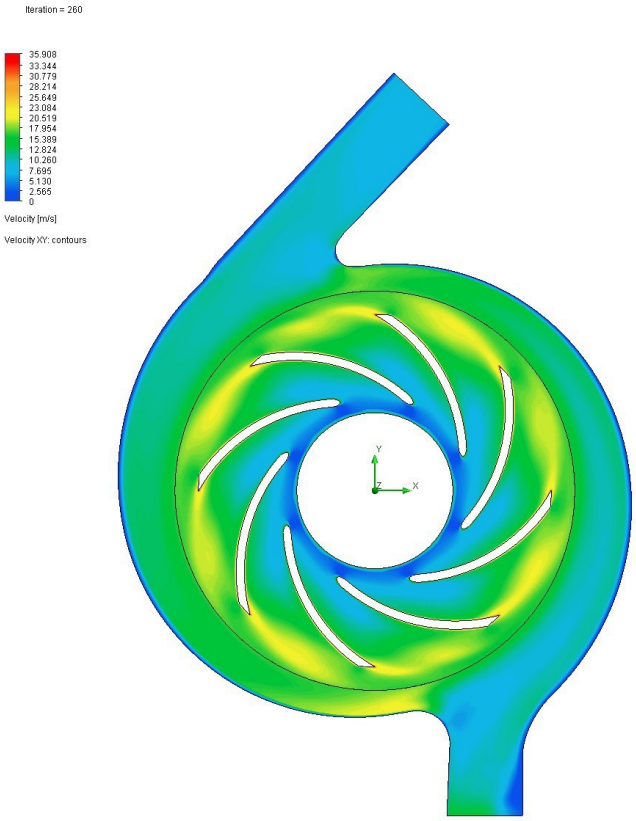

Figure 64: Velocity plane XY

This scene shows why the asymmetric geometry causes the reduction in the flow to the B bank. Some other interesting bits are the two stagnation points, again dark blue, in the narrowest section before the outlets. These two could cause detachment and vortices in the outlet flow.

- **Velocity plane XZ**

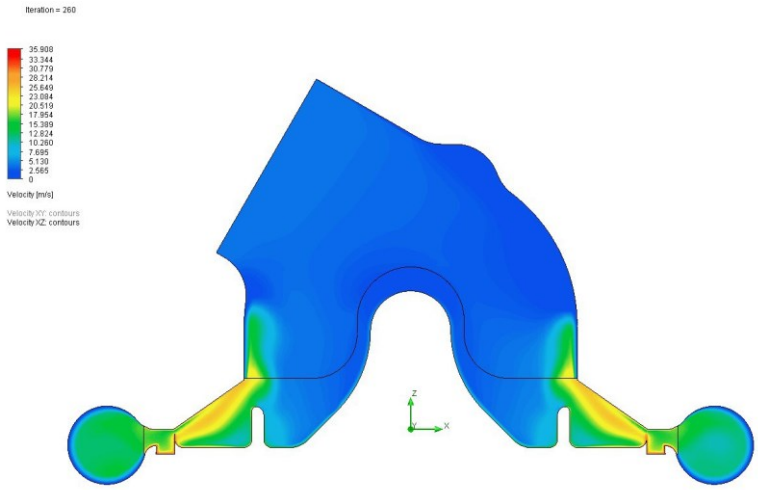

Figure 65: Velocity plane XZ

This image does not add much except the velocity gradient between the impeller vane and the main channels.

- **Pressure plane XY**

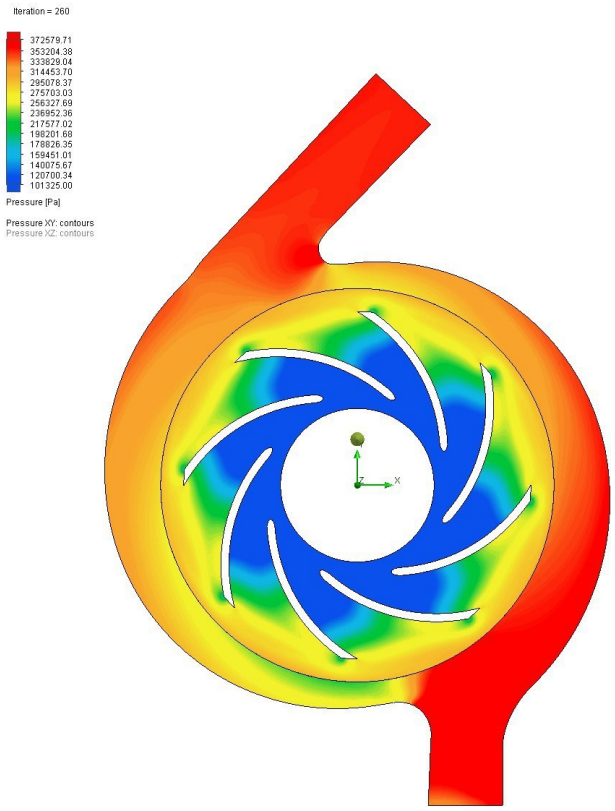

Figure 66: Pressure plane XY

The pressure scene is complementary to the velocity one. It allows to better understand the pressure differences inside the vanes, as mentioned in the velocity scene, a proper pressure rise is recorded along the outlet ducts. It is now easier to visualise the stagnation points (on the upper side and so the A bank outlet) where the colour gradient changes from red to orange. The situation is slightly different on the B bank exit where the pressure is average higher causing a massive pressure drop (see first section of the vane) which, again, could be the cause of turbulences not allowing a fully developed profile and a reduction in the flow percentage.

- **Pressure Plane XZ**

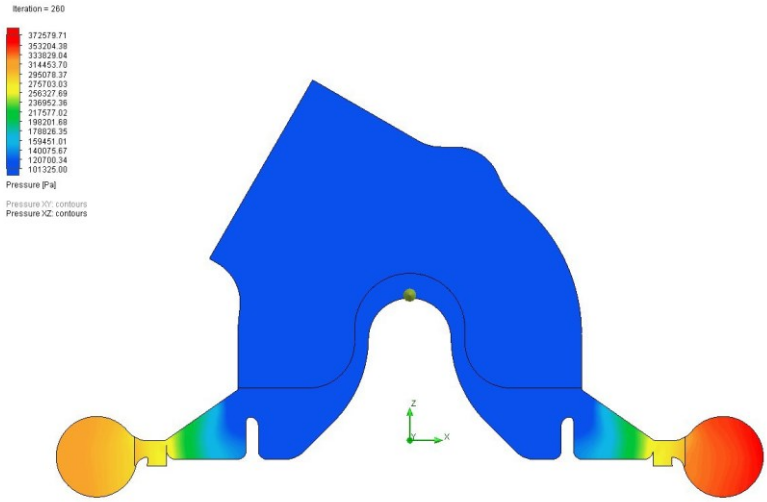

Figure 67: Pressure plane XZ

This scene does not say much more than the previous one but it helps us to visualise the gradient between the inlet section and the vanes.

- **Temperature plane XY**

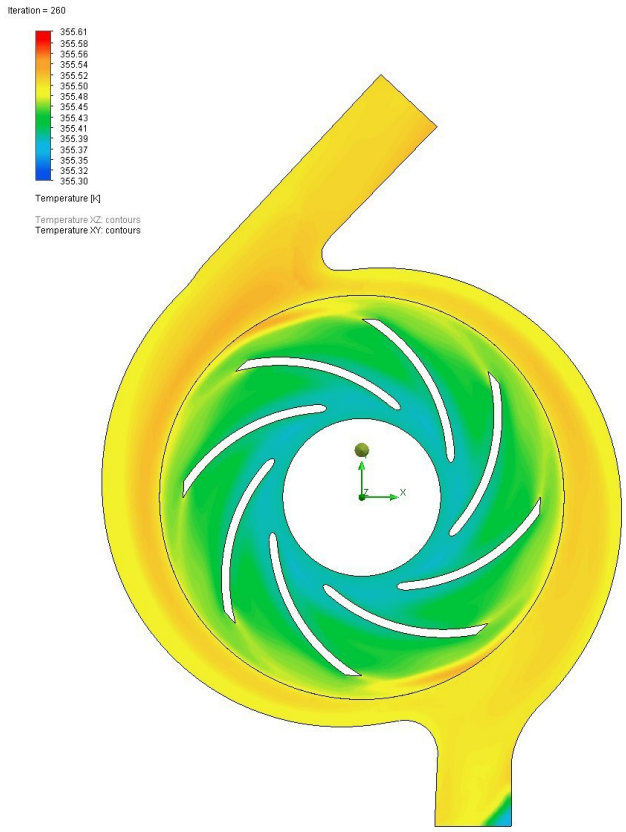

Figure 68: Temperature plane XY

- **Temperature plane XZ**

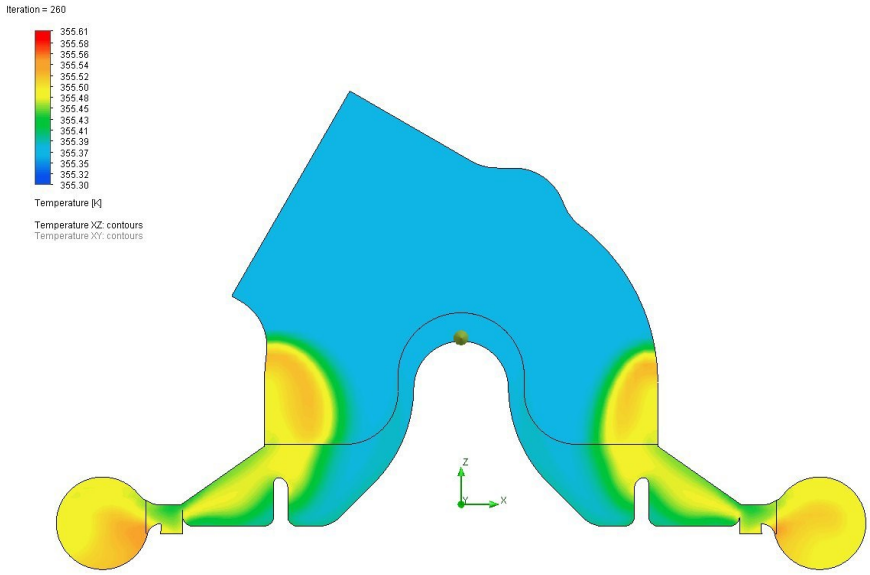

Figure 69: Temperature plane XZ

These two images could be avoided since the temperature is pretty much constant in the whole domain, but they give a complete description of the fluid moved inside the pump.

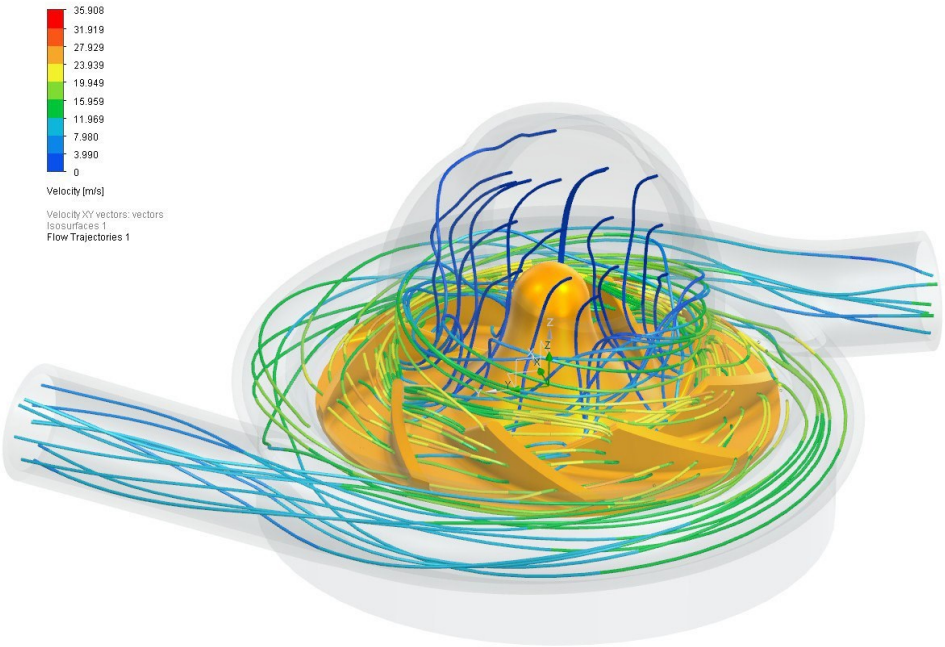

Figure 70: Pump streamlines

8.4.2 Comments on the numerical results

The numerical results are now reported starting from the flow through A bank and B bank outlet.

Simulation	Flow A	%	Flow B	%	Total
1	4.8941	53.84553	4.5142	49.66582	103.5114
2	5.062	55.69279	4.1809	45.99881	101.6916
3	4.9009	53.92035	4.2628	46.89989	100.8202
4	4.8835	53.72891	4.2067	46.28267	100.0116
5	4.9736	54.7202	4.1728	45.90969	100.6299

As we can see the simulation did probably not reach the fully convergence, but, as mentioned, this was enough for what was our goal. The main reason for this simulation was to show the feeding difference between the two sides to evaluate Packard's paper and we are more than happy since the flow to the B bank is 45.91% instead of 47%. We than have to keep in mind that we used values from TSD 83 and Packard's tables which, of course, causes some slightly differences in the final results. Furthermore, it has been interesting to show the reason for this as already explained using the graphic scenes where the asymmetric ducts cause flow detachment and recirculation bubbles chocking the B bank outlet. From simulation three to five we only have fluctuations smaller than 1% which are acceptable.

One last note regards the last column where the total flow is higher than 100%, this could be easily explained since a rotating region is defined. Sometimes if not well refined the interface between that and the static side could be the cause of small errors in the equation's resolution. Results can be improved refining the mesh in the region but, on the other hand, the computational cost increase drastically.

It has then been decided to simulate the worst-case scenario where the reference value of flow used in the upcoming cylinder bank simulation is highlighted above. The *Velocity* has been properly measured over this outlet and it is 8.024 $\frac{m}{s}$ while the *Absolute Pressure* measures 318419.8 Pa.

8.5 B bank complete flow simulation

With the pump simulation finalized and all key results documented, we are ready to transition to the next task: the simulation of the flow through the entire B bank. The aim of this second simulation is to get some initial result regarding the flow behaviour inside the cylinder head and skirts. This will point out critical spots inside the same jacket and will give us the “basis” to find out appropriate solutions for the problems occurring with this Hurricane’s configuration.

Being this simulation much more complicated than the previous one it has been decided to extract the entire water jacket inside NX environment and then define a “big block” to simulate the solid bodies such as cylinder head, cylinder banks and rail. It is probably not the best-looking option but definitely the best if we think about the functionality of the model. What is more extracting the inner volume from the original CAD into FloEFD environment parts would require an high computational cost being the geometry very detailed.

Many control “planes” and “points” have then been defined, in order to capture the velocity, the mass flow, and the shear stresses in critical regions of the water jacket.

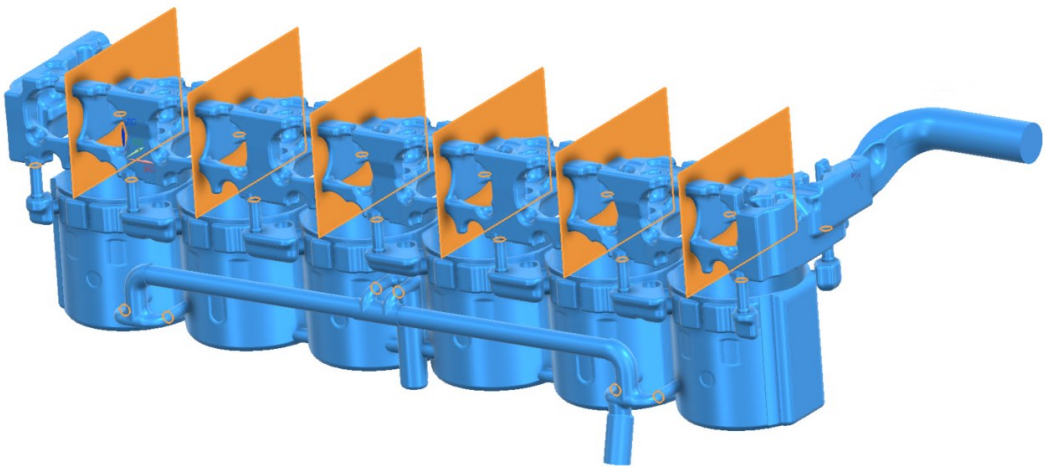

Figure 71: Control points and planes

As visible in the image above six planes and twenty control points (coloured in orange) have been created in all the important passages.

The cylinders are named from “one” (back of the engine) to “six” (front of the engine) as the planes between the exhaust ports.

The “flow control points” on the rail are named from “one to “six” from the front to the back.

The “flow control points” between the skirts and the head are named from “one” to “seven” on the inlet side and “eight” to “fourteen” on the exhaust side from the front to the back.

All these little pieces of geometry have been created inside NX environment to facilitate their definition.

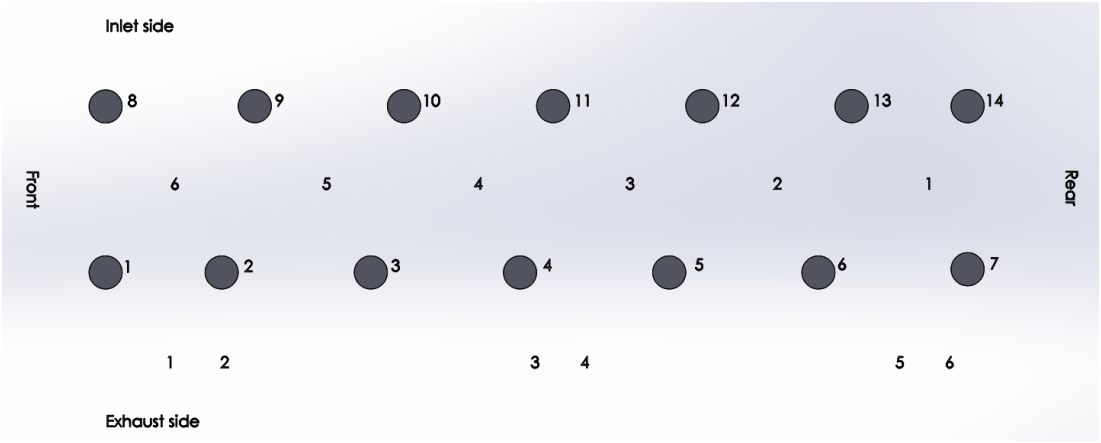

Figure 72: Control points schematic map

It is now possible to move to the “FloEFD” environment since the geometry, with all the important planes and points have been defined.

Boundary and initial conditions could now been set starting from the output of the previous pump simulation.

Boundary conditions

- **Mass flow inlet** in the rail where the flow is $4.1728\ \frac{kg}{s}$;
- **Pressure outlet** on the coolant elbow where the pressure is set to $270156\ Pa$. This value has been tabulated starting from the pressure obtained on the B bank pump outlet minus the pressure losses defined into an old Packard’s report.

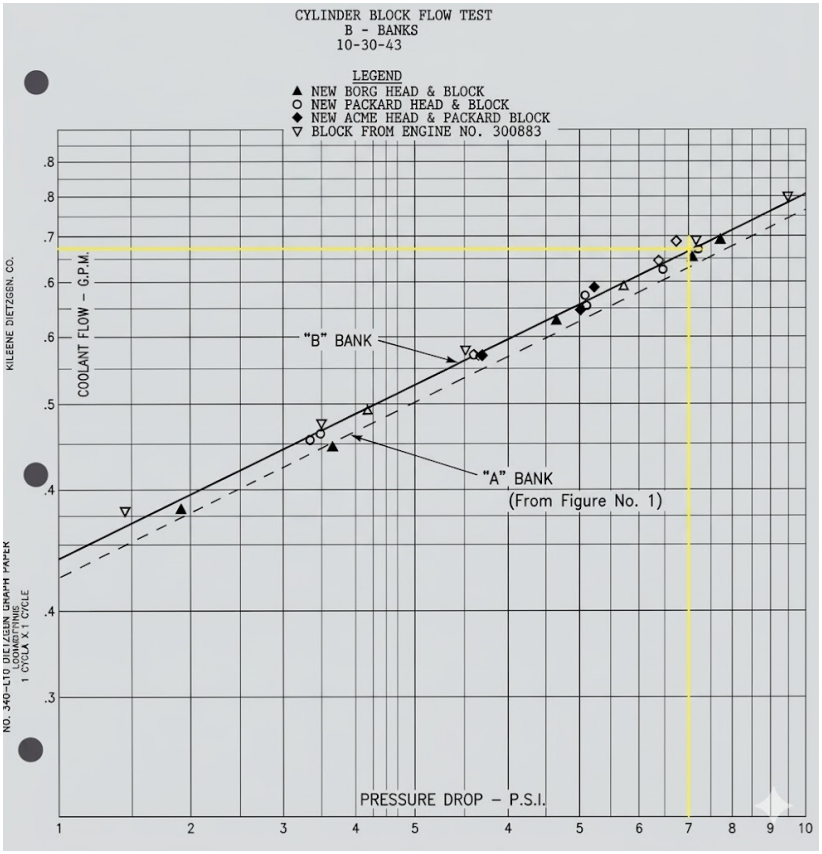

Figure 73: Pressure losses in the cylinder block and head

We converted our mass flow value to US gallons. The calculation gave us $67.266\ Us\ Gal$ which (see yellow lines above) correspond to a pressure drop of $7\ PSI$, or $48263.3\ Pa$.

No more boundary conditions were defined.

Initial conditions

- $T = 355.372\ K$;
- *Turbulent kinetic energy*

$$k = \frac{3}{2} u'^2 = \frac{3}{2} * 0.8024^2 = 0.96577\ (\frac{m}{s})^2$$

The value for u' is given by the following equation

$$u = T.I. * u' = 0.1 * 8.024 = 0.8024\ \frac{m}{s}$$

- $T.I.$ is the "Turbolence intensity" and is assumed 0.1;
- u is the "inlet velocity" which we remember being $8.024\ \frac{m}{s}$;

- *Turbulent dissipation rate*

$$\varepsilon = C_{\mu}^{3/4} \frac{k}{TLS}^{3/2} = 0.09^{3/4} \frac{0.96577}{0.0028956}^{3/2} = 53.858 \frac{m}{s}$$

Before the generation of the mesh many reports have been created to get a proper value of flow through each passage showed in *Figure 69.* Some additional surface plots are added to analyse the Shear Stresses in the little passage between the exhaust valves. Shear Stresses are a very important parameter in fluid-dynamics, they represent internal friction forces caused by velocity gradients in a fluid, calculated as

$$\tau = \mu \frac{\partial u}{\partial y}$$

and for Newtonian fluids measured in $\frac{1}{s}$. Where:

- μ is the *Dynamic Viscosity* which is measured in $\frac{kg}{m\,s}$ and, as already showed, is a property of the fluid;
- $\frac{\partial u}{\partial y}$ is the *Velocity Gradient* of the fluid and represent the rate of change of velocity perpendicular to the direction of flow.

It is now easy to understand why this term is so important. Force convection is the most important way to transfer heat from the engine to the water jacket and another important parameter to evaluate this phenomenon is the *"Heat transfer coefficient"*

$$h = Nu \frac{k}{L}$$

Where:

- Nu is the "*Nusselt Number"* a non-dimensional parameter which identify the correlation between the conduction and convection heat exchanges. This parameter is often expressed as:

$$Nu = C * Re^{m} * Pr^{n}$$

In which $\boldsymbol{Re}$ is the "*Reynolds Number*" a non-dimensional parameter which express the correlation between the "*Momentum terms*" and the *"Viscous stresses"* displayed into the "*Navier Stokes Equations*". $\boldsymbol{Pr}$ is the *"Prandtl Number"* defined as the correlation between the "*Kinematic viscosity"* and the "*Thermal diffusivity"*.

- k is the "*Thermal Conductivity"* expressed in $[\frac{W}{mK}]$;
- L is the "*Reference Length"* $[m]$.

The mesh could now be generated. A very rough first attempt was made using the function "Automesh" set to level 5. The total number of cells was 102000. The geometry was very badly defined and distorted but was aimed to show criticisms and problems in the model which we avoided.

The results were very approximate but gave us a first taste of the general behaviour of the coolant.

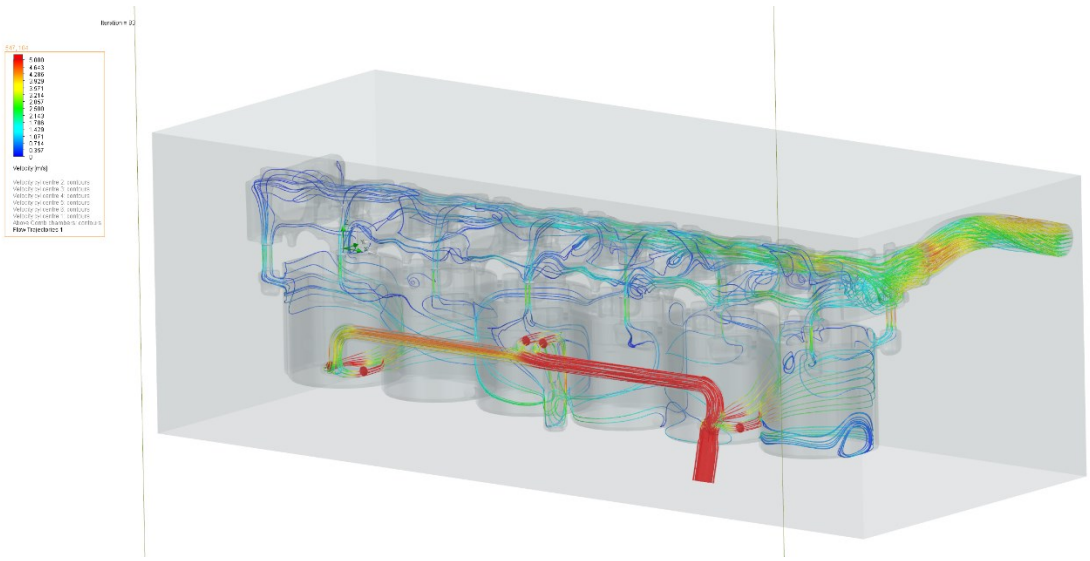

Figure 74: Streamlines first simulation

It is easy to imagine what we can expect from now on. As shown there is a general tendency for the velocity to reduce from cylinder one to six and, as consequence, the heat exchange.

As for the pump, many other simulations have been run. All the important setting were as follow:

- **Second simulation**
    - Automesh level 5;
    - Four “boxes” for refinement have been defined in all rail and head passages where fluid cells were set to refinement level three as the fluid-solid ones. The curvature inside the same boxes have been set to level one.
    - Total 207450 cells.
- **Third simulation**
    - Cells size set manually to 0.0125 m along x, y and z axes. Additional small channel cells set to 25 with refinement level three;
    - The four boxes were set as in the previous simulation;
    - Total 694849 cells.
- **Fourth simulation**
    - Cells size set manually to 0.011 m along x, y and z axes. Additional small channel cells set to 30 with refinement level three;
    - The four boxes were set as in the previous simulation;
    - Total 924823 cells.
- **Fifth simulation**
    - Cells size set manually to 0.011 m along x, y and z axes. Additional small channel cells set to 30 with refinement level three;
    - The four boxes were set as in the previous simulation except for the curvature level which have been increased to level two;
    - Additional spherical refinement defined in the outlet elbow with the same levels defined in the four boxes previously described;
    - Total 1118804 cells.
- **Sixth simulation**
    - Cells size set manually to 0.011 m along x, y and z axes. Additional small channel cells set to 30 with refinement level three;

- The four boxes were set as in the previous simulation except for the curvature level which have been increased to level two;
- Additional spherical refinement defined in the outlet elbow with the same levels defined in the four boxes previously described;
- Six boxes to increase the refinement between the exhaust valves where fluid cells were set to refinement level four as the fluid-solid ones.
- Total 2030751 cells.

Being this a preliminary analysis and graphical simulation we decided to stop. We could have go on but the main goal, again, was to show the general behaviour of the flow and highlight the weaknesses of the configuration adopted by the BBMF Hawker Hurricane. Many interesting considerations could be done form the following reports and images. Some possible solutions will be then reported at the end.

8.5.1 Graphic scenes

The results of the simulation six are then shown below.

- **General mesh**

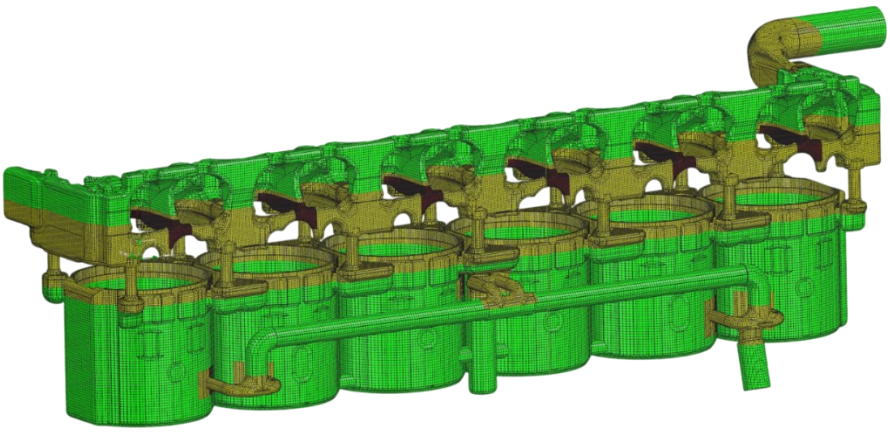

Figure 75: Global mesh

The mesh is displayed and, as mentioned above, many refinements have been introduced in all the important passages (orange) and between the exhaust valves (red).

- **Shear stresses**

Shear stresses are now displayed. These images are remarkably important for the understanding of the velocity and mass flow plots which will then be shown below.

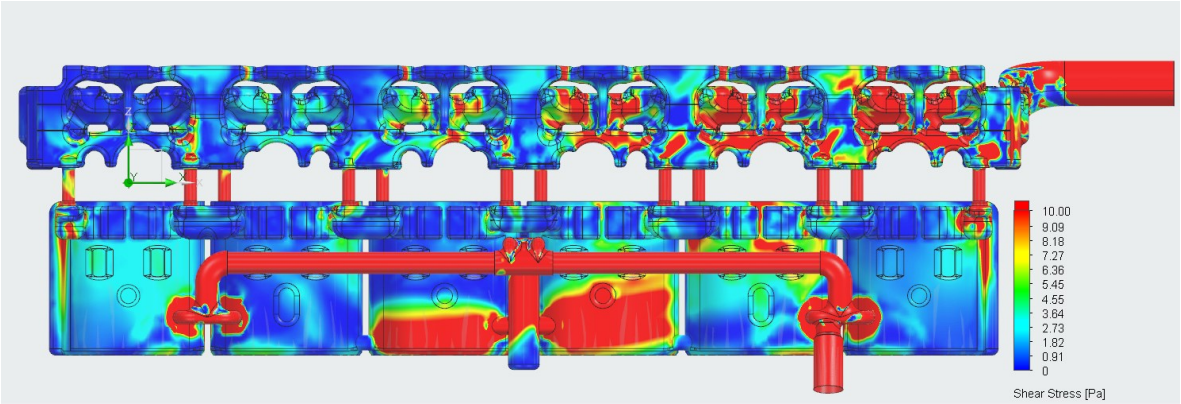

Figure 76: Shear stresses exhaust side

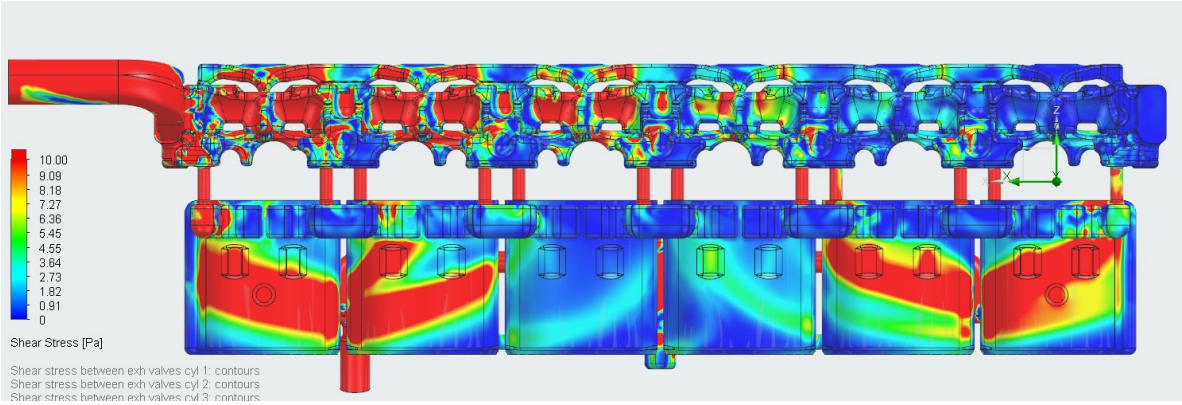

Figure 77: Shear stresses intake side

These two images could be enough to understand the overheating problems occurring inside the Hurricane's Merlin 500. The upper value of the scale has been set to 10 Pa as a reference. It is a quiet low value but definitely enough as a first instance since many studies consider this number enough to avoid stagnation and localised boiling spots. We can easily see how the fluid velocity tents to decrease after the first rails passages. This is massively caused by the same water feeding system configuration which was meant to hit tangentially the region between the liners and the cylinder block creating a sort of "swirl" in the region. The configuration guarantees a good velocity gradient on the exhaust side for cylinders one, two, five and six but on the other hand, almost

zero on three and four. The situation is the exact opposite on the exhaust side where cylinders three and four are well cooled compared to the other four.

Moving upwards some considerations could be done for the passages between the cylinders and the head where the gradient decreases moving from cylinder one to six. This is the cause of water stagnation in the head from cylinder three to six. The obvious reason for this is the shortcut the water follows being the feeding on the same end as the exit.

It is now possible to analyse the head and, in particular, the exhaust valves region where the colours displayed underline how the shear stresses move from high (cylinder one) to lower (cylinder six) values. The values are even lower if we look at the tiny bridge between the exhaust valve seats.

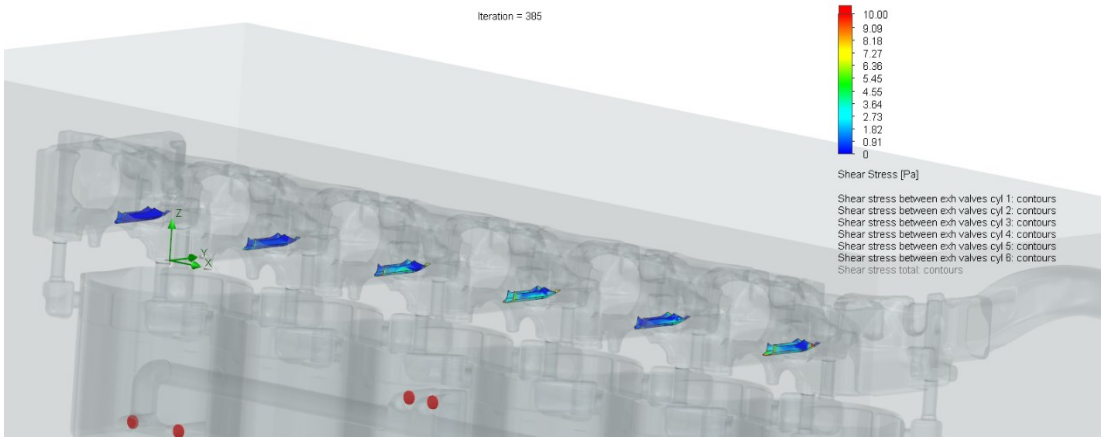

Figure 78: Shear Stresses between exhaust valve seats

The region between the two exhaust valves is one of the hottest and most critical inside an engine because of the huge amount of heat expelled through the same passages after a combustion. It should be reasonable to have high values of Shear Stresses but as shown in *Figure 75* the average value is way lower than the maximum set, 10 Pa. This is of course a huge problem since the region is mechanically loaded too having steel valve seats which are cause of compression stresses in the same region. Studying different drawings from different periods has pointed out how Rolls-Royce tried to, partially, solve the problem introducing, for instance, a slot which aimed to reduce the thickness of the region allowing more water to going through but, as visible below, the fluid is almost stagnant everywhere.

Figure 79: Shear Stresses between exhaust valve seats bottom view

As mentioned previously low Shear Stresses mean low velocity gradient and, consequently, low heat exchanges. It is now easy to understand why this rear-end mounting elbows could be a cause of overheating for the Merlin 500 when mounted into BBMF's Hawker Hurricane.

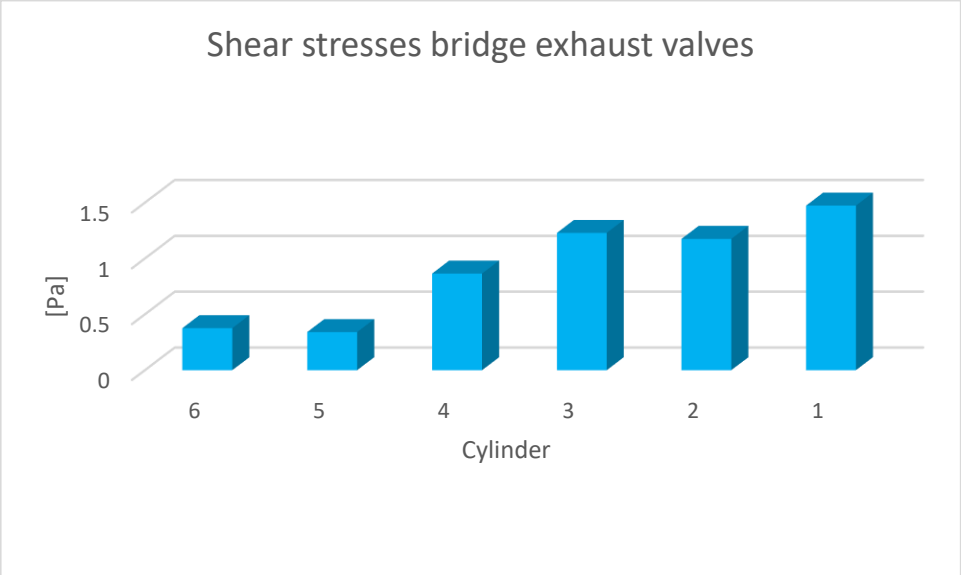

The average value of "*Shear Stresses"* are here reported. As underlined the values are lower than 2 Pa and gradually decreases from cylinder one to six.

- **Velocity scenes**

Having analysed the viscous Shear Stresses give us the opportunity to look at the velocity scenes.

We point out that has been decided to focus on the region between the exhaust valves and on the place above the combustion chamber, being as already mentioned, the most critical zones.

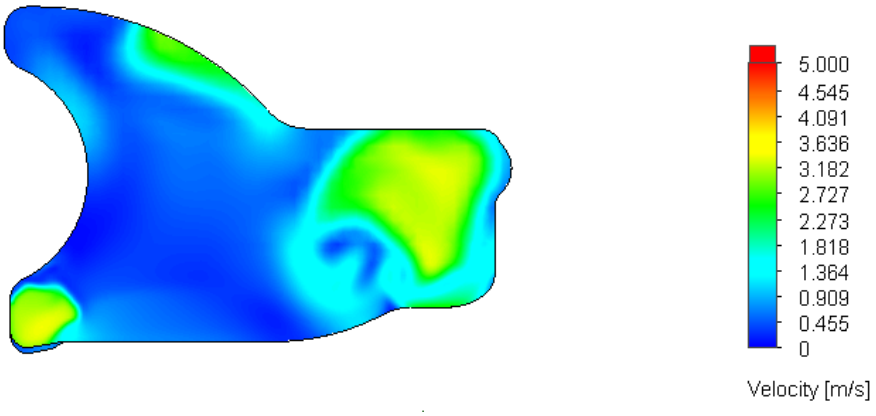

Figure 80: Average velocity between exhaust valves cylinder one

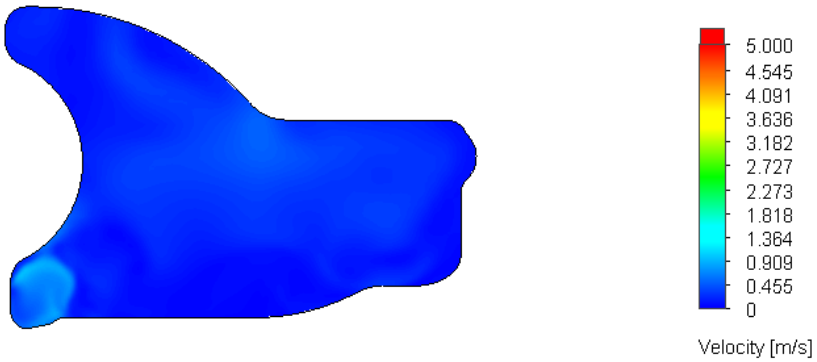

Figure 81: Average velocity between exhaust valves cylinder six

Figure 80 and *Figure 81* show this phenomenon quiet well. The difference in terms of velocity gradient on the plane between the exhaust ports in cylinder one and six is remarkable. In both cases the average value is lower than 3 $\frac{m}{s}$ even if in cylinder one is easy to see many spots where the values is higher than 4 $\frac{m}{s}$. Anyway the average value in the bridge between the valves is lower than 2.5 $\frac{m}{s}$.

The same situation could be seen in a plane above the combustion chambers.

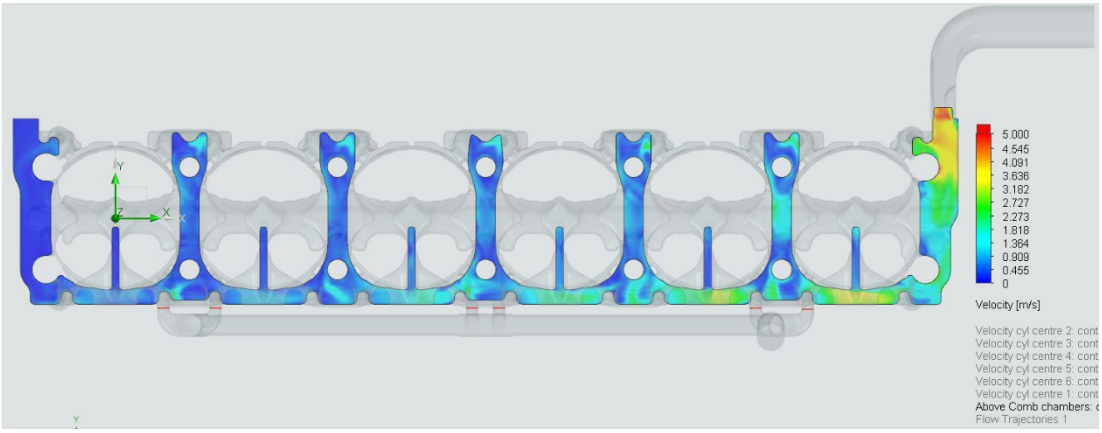

Figure 82: Average velocity above the combustion chambers

The trend is visible in the plane above the combustion chambers where we find values lower than 2 $\frac{m}{s}$ more or less everywhere except in the proximity of the outlet and between the exhaust ports in cylinders one and two. The situation is critical even among the combustion chambers where the only cyan spots identify the head feeding passages.

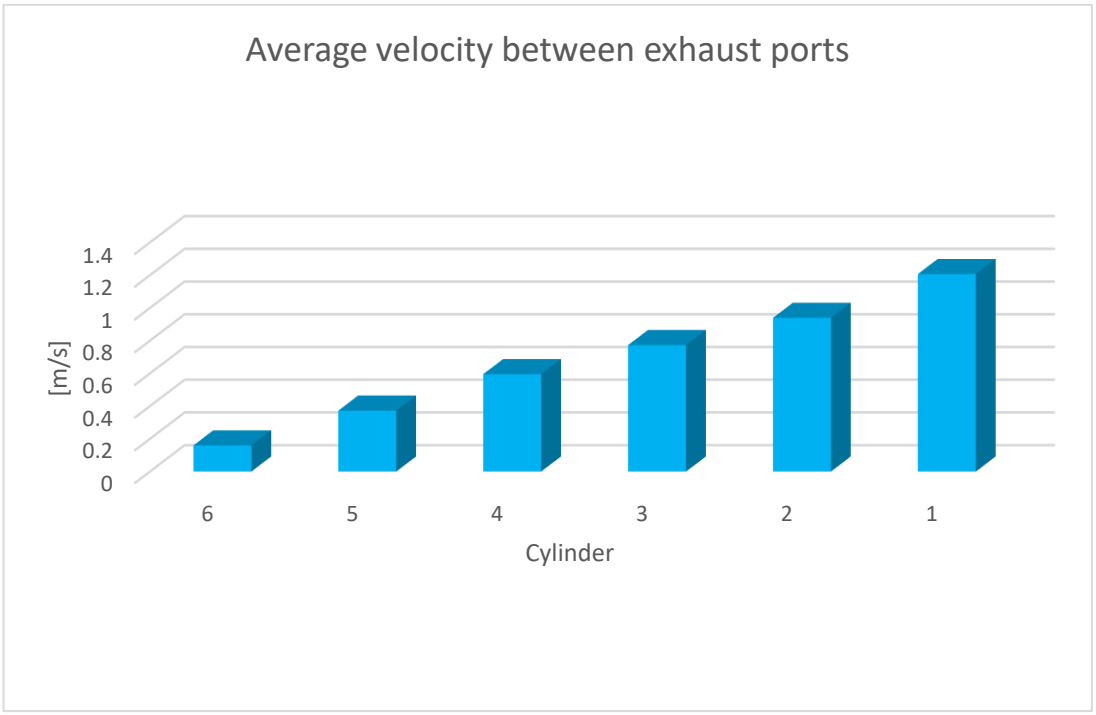

As visible from the graphic above the general trend is reflect what we have already analysed with the Shear Stresses. The average velocity tends to decrease between cylinder one to six.

- **Pressure scenes**

We can now complete the description of the flow above the combustion chambers with the pressure scene. It is easy to see higher values moving to the last cylinders where the water is more or less stagnant compared to the first ones which are closest to the pressure outlet.

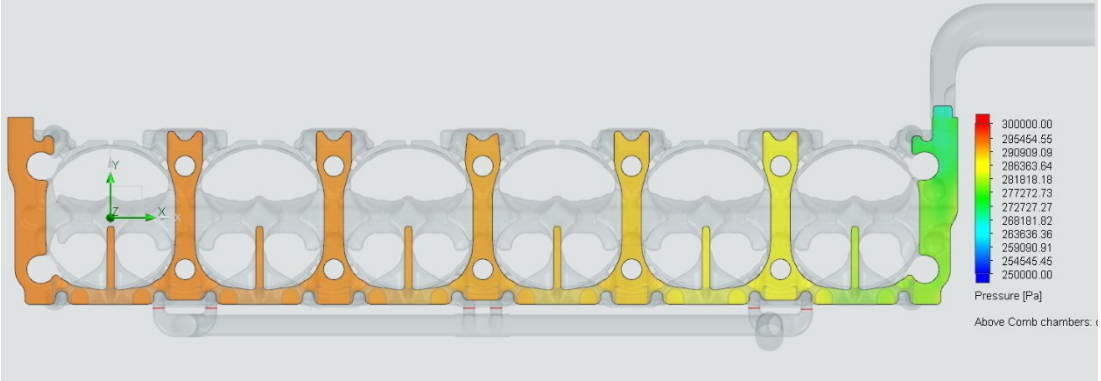

Figure 83: Pressure above combustion chambers

- **Mass flow through the passages**

The mass flow through the passages are now reported giving us a physical visualisation of the imbalance of water passing through each connection. The first chart below shows the water passing from the rail to the skirts.

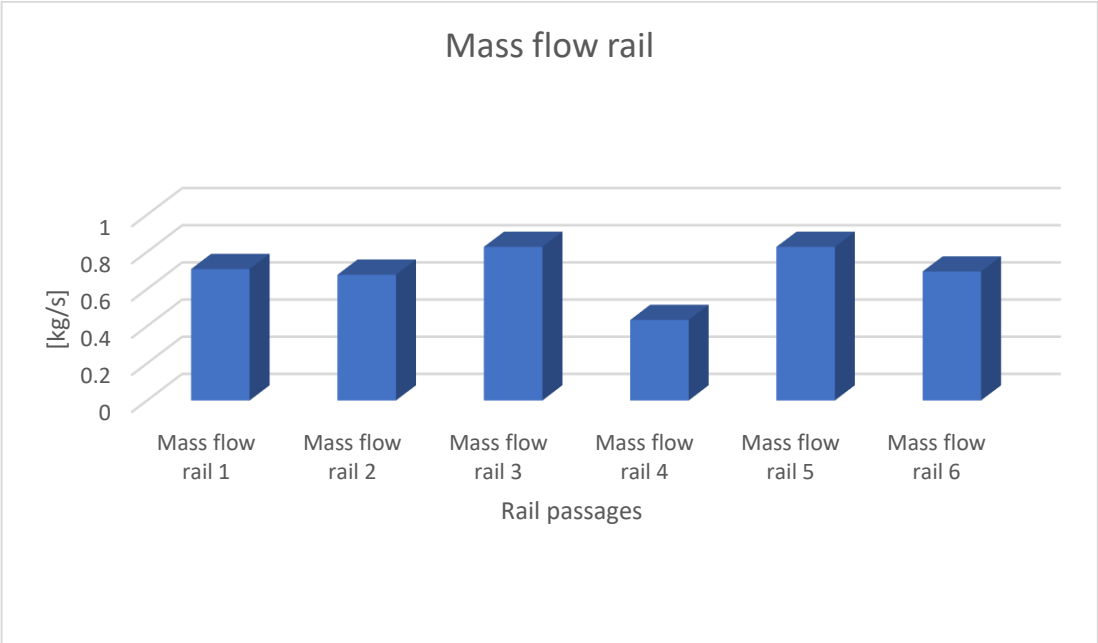

The general trend underlines how the passages one, two and five, six are generally balanced compared to the central ones and this is for obvious reasons. The first ones are the easiest to be feed while the last suppose that the fluid, as soon as it reaches the end, passes anyway. The central ones, those which supply cylinder three and four, are the most disadvantaged since the fluid needs to turn while pushed by the amount coming from the pump. It gets just 10% of the total fluid, which compared to the other ones is way lower since they all attest between 16% and 19%. This concept will be much easier to understand as soon as the streamlines will be shown below.

Moving on another very interesting graph is the one now reported where we dispose the column as in the *"Figure 69"* to give a real feeling of the imbalance through the head passeges.

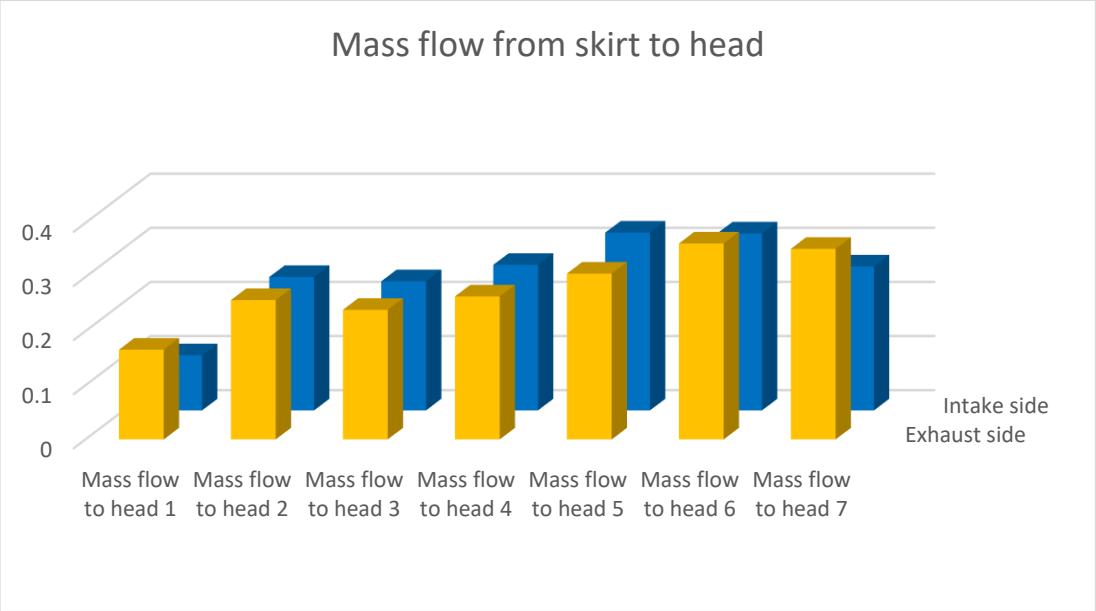

Personally, I find this chart very useul from many points of view. At first instance, as mentioned, gives us a clear visualisation of the imbalance of the flow going from the skirts to the head and, again, is clear that the most disadvantaged cylinders are the last ones. The amount of flow decreases in a linear way from the passages closest to the rear of the head to the one in the front, except for the passage fourteen. This is because of intense vortices on the outlet passage of the head, where the elbow is connected. This detail will be shown later on. The least fed passage is the number eight which is the most

distant from the pump, it gets about 2.4% of the total flow, while the one with the highest flow is the number six with 8.7%.

- **Streamlines scenes**

Streamlines scenes are now displayed. These last images will conclude the complete description of the flow behaviour inside the cylinder head.

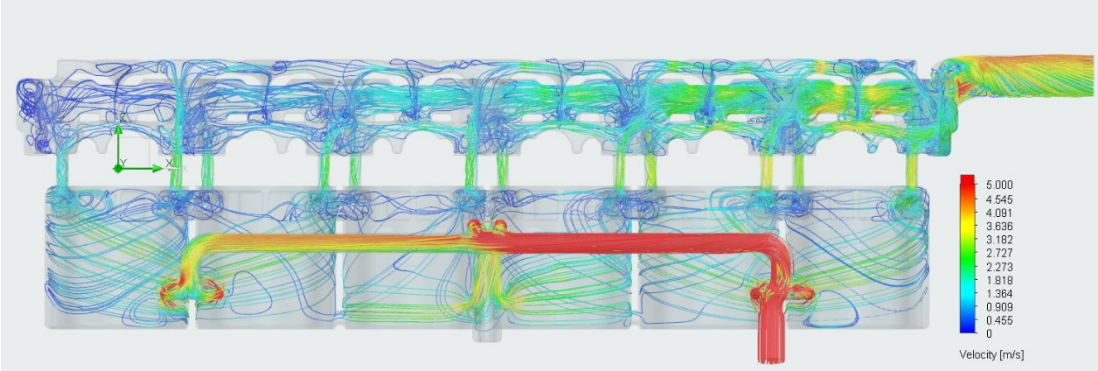

Figure 84: Streamlines exhaust side view

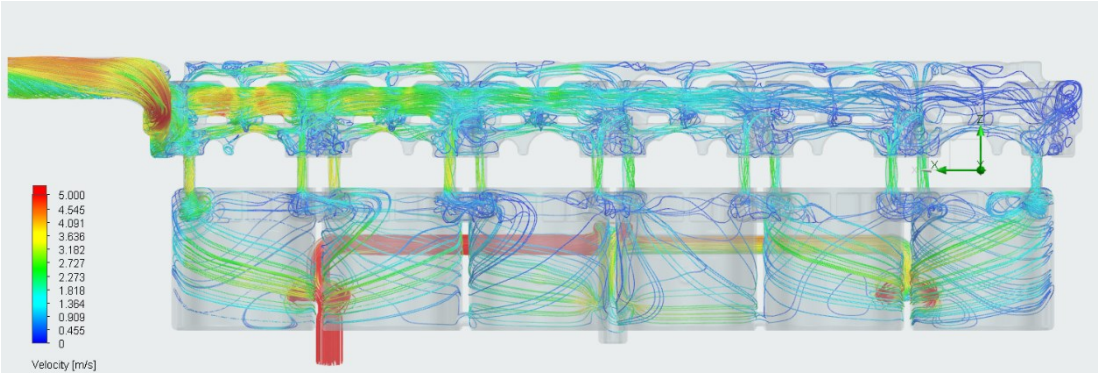

Figure 85: Streamlines intake side view

These to images defines once for all the flow from a visual point of view. It is now possible to see the swirl on the cylinder skirts and the difference in terms of velocity in the various sections along the model. A massive velocity drop could be seen on the intake rail where, from half way in, the average speed decrease from more than 5 $\frac{m}{s}$ to 3.5 $\frac{m}{s}$. It is also possible to see how distorted and turbulent the flow is inside the little pockets located in the cylinder skirts mostly because of the presence of the main studs which partially cover the inlet passages. Other interesting considerations regards the cylinder head where massive recirculation are spotted on the last cylinders. Moreover the

blue colour identifies stagnation and, so, weak regions where could be easy to find cracks.

Some small considerations over two interesting regions are now reported. We have already mentioned and displayed that the passage number fourteen defines a lower mass flow compared to the other passages in the first three cylinders. Here is the reason why. It is now possible to see how a massive eddy “choke” this outlet allowing a lower mass flow to go through. Even though the outlet defines a restriction and, with so, a higher velocity of the flow, a small stagnation region is easy to spot just below the same port. Moreover the same passage is characterised by a turbulent flow compared to the “laminar” we can easy see on the others. One last interesting detail is the recirculation bubble before the outlet curve where the flow is again, chocked and distorted.

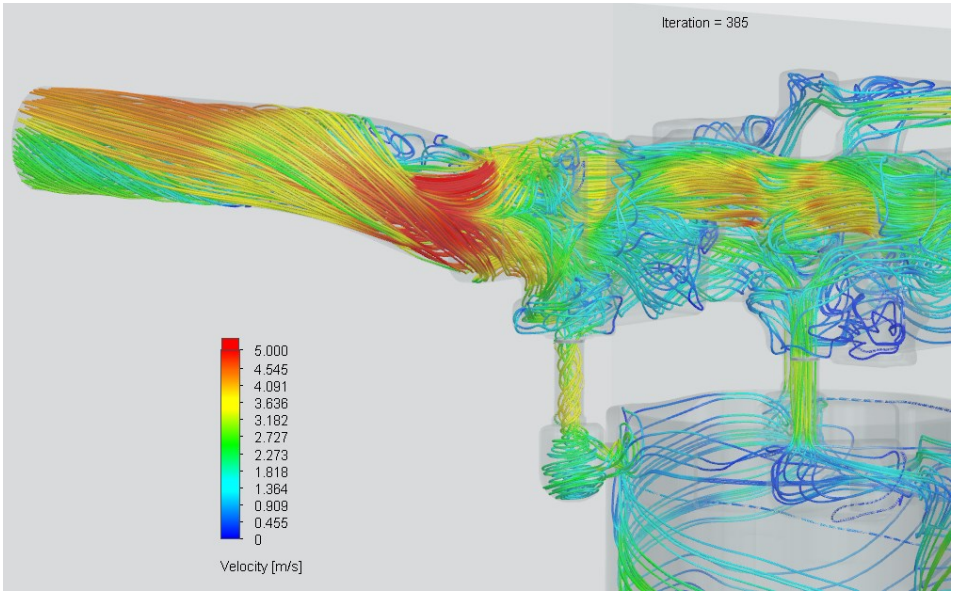

Figure 86: Outlet elbow detailed view

One last detail we would like to focus on is the inlet rail which, as mentioned, is defined by an intense velocity gradient along the same. What is more a very twisted flow is defined in the passages which bring the fluid to the skirts. The flow is here twisted and so distorted even though, at least for the passages number five and six, it hits tangentially the liners as it is supposed to. A quiet different situation is found on the passages three and four where the swirl but also the velocity is “cancelled” by the geometry. The presence of the central main stud distorts and slow down the fluid which enters the liners quiet slowly.

One last bit could be analysed. Passage number four is characterised by the lowest mass flow possibly because of it position which lets the flow to move to other passages.

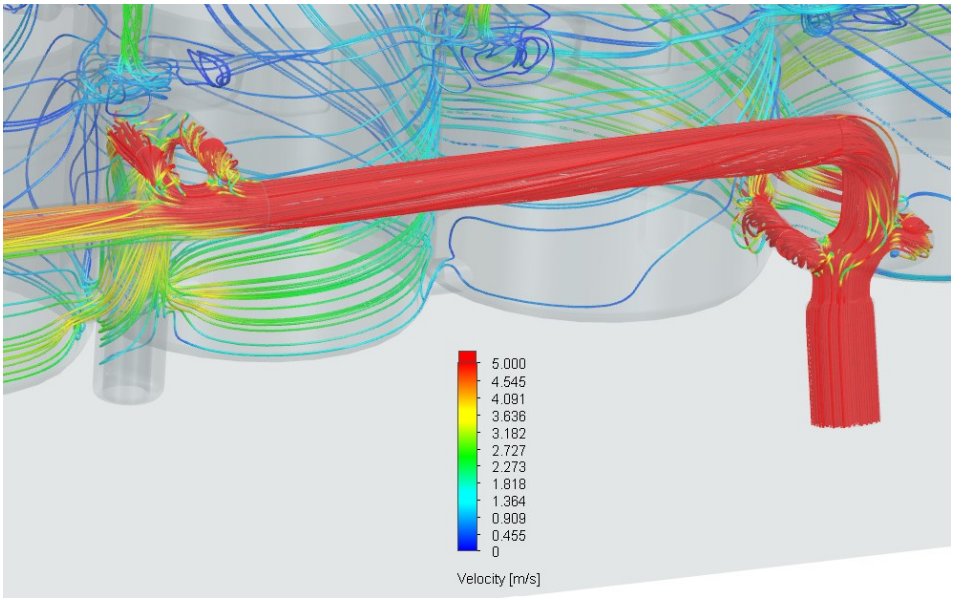

Figure 87: Inlet rail detailed view

8.5.2 Possible solutions

The problem presented in the pages above is something that needs to be corrected as soon as possible to avoid trashing more cylinder heads after each overhauling of the engines. Unfortunately the time I had did not allow me to complete the study with updated versions of the cooling system. Some solutions have anyway been found. Below a list from the easiest to the most difficult one.

- **Inlet rail sizing**

The first and easier solution requires to work on the size of the rail passages. A reduction in the diameter will possibly force an higher amount of flow to the further cylinders, four five and six, and of course a better recirculation inside the head since the path that the water have to follow is always the same. This will anyway guarantee the flow to hit the first cylinders allowing, in theory, good values of Shear Stresses because of the outlet elbow location. Some simulations will then be required to tune opportunely the model.

- **Head feeding inlet**

The same procedure could be applied to choke or enlarge the small passages that connects the skirts to the head. It is likely that three or four size of passages will be needed. Again, some simulations will than be required to equally spread the flow through the head.

- **Front rear-faced coolant elbow**

This could probably be one of the best solutions since the same Merlin 500 have been developed this way. The problem will probably be to design the correct elbow because of the Hurricane's header tank position, which we remember to the readers, is located on the back of the engine. The configuration of the Mustang P-51H could be used as a reference since the cooling system configuration is similar to the Hurricane's.

9. Conclusions

Reverse engineering does not mean copying a geometry because a model is needed for any purpose, it is much more. Starting from eighty years old drawings, ending up with a proper CAD model and then a real component which will be fit into an airworthy airplane is something else. This was a massive project to be done in such a short time, moreover with almost zero knowledge of 3D modelling. It gives me the opportunity to learn how to design massive components with very clean and organised CAD models. The use of solid features, the surfaces and the Boolean operations represent the complete set which every designer should know and this project was the perfect chance to learn and experiment them all. The use of these functions is not the only important lesson learnt but also the research for the best, and I would say easiest, way to realise any feature. Sometimes you can design using solids, sometimes you must use surfaces, sometimes both.

The definition of casting and machining models also gave the opportunity to interface with external company, as the foundry, and our machine shop. This makes you thinking “out of the box” since sometimes there are features, components or processes that are fine while using NX but not when somebody have to realise them.

Another important lesson achieved is the understanding of big drawings, being able to interpret big sheets plenty of small details and features allows to imagine a components and features even before designing them inside a CAD environment. The analysis of the sections and the views is also important because allows to search for errors or missing constrains which are usually crucial for a fully definition of the model.

Drawing but also historic documentation and imperial system values, charts and diagrams. All this information have been crucial for the late CFD simulations at first for the pump and, consequently, for the complete cylinder bank. Simulation and problem visualization would have not been possible without proper models, because in addition to the cylinder head, all the other components have been modelled.

A good simulation requires good models which are not always available because design and simulation are often assigned to different departments. Having the possibility to change, adapt and modify your own model is largely important because gives you the ability to fully control what you are doing. Sometimes frustrating but rewarding mostly when the results finally give you the chance to visualise the problems occurring inside the water jacket. For the first time since BBMF fit Merlin 500 inside Hurricane has been possible to highlight one of the main causes of cracks in the cylinder head showing that the problem was not the elbow but its mounting position. It will now be feasible to complete the project introducing modifications to the feeding system as discussed above as first instance and then, eventually, to change the skirts design. Further CHT simulations will be needed to analyse the iteration of the fluid and the cylinder head, but also the steel valve seats giving a complete fluid-dynamic assets of the engine.

10. Bibliography

- **Chapter 1**:

[1] *"Merlin, the power behind the Spitfire, Mosquito and Lancaster"*, Graham Hoyland, William Collins

[2] https://en.wikipedia.org/wiki/Rolls-Royce_Limited

[3]https://www.press.rolls-roycemotorcars.com/rolls-royce-motor-cars-pressclub/article/detail/T0454168EN/rolls-royce-heritage:-from-1904-to-today-%E2%80%93-and-beyond?language=en

- **Chapters 2 and 3**:

[4] https://www.raf.mod.uk/display-teams/battle-of-britain-memorial-flight/

[5] https://en.wikipedia.org/wiki/Royal_Air_Force

- **Chapters 4 and 5**:

[6] *"Not much of an engineer"*, Sir Stanley Hooker, Airlife

[7] *"The secret horsepower race"*, Calum E. Douglas, Tempest Books

[8] *"Supermarine Spitfire Restoration Manual"*, Paul and Louise Blackah, Haynes

[9] *"Hiduminium RR50 General purpose sand and die casting alloy"*, Air Ministry Specification D.T.D. 133B

- **Chapter 6**:

[10] https://www.sw.siemens.com/en-US/technology/reverse-engineering/

- **Chapter 8**:

[11] "*Packard V-1650 Report No260 V-1650-9 Cylinder Bank Coolant Flow Test"*

[12] "*Packard V-1650 Report No169 Heat Rejection and Coolant Flow Characteristics of V-1650 Two Stage Engines"*

[13] *“V1650-3 Engine B-6 Test at Emergency Power Rpt-126-Emerg_Power_Tst_Cover_Index_p1of2_0001”*

[14] *“Packard V-1650 Report No145 (draft) Coolant Pump Test Summary”*

[15] *“Packard V-1650 Report No180 Cylinder Head Temperature Survey on V-1650-3”*

[16] *“TSD 83 Merlin 24 & 500 Series performance and installation data”*

[17] Monoethylene-Glycol-MEG-Technical-Product-Brochure-PDF.pdf

[18] EGL.pdf

11. Figure index